Development in electrophoresis: instrumentation for two-dimensional gel electrophoresis of protein separation and application of capillary electrophoresis in micro-bioanalysis

by

Aoshuang Xu

A dissertation submitted to the graduate faculty

in partial fulfillment of the requirements for the degree of

DOCTOR OF PHILOSOPHY

Major: Analytical Chemistry

Program of Study Committee:
Edward S. Yeung, Major Professor
Robert S. Houk
Victor S.-Y. Lin
Emily Smith
Louisa B. Tabatabai

Iowa State University

Ames, Iowa

2008

To my beloved Grandma

TABLE OF CONTENTS

CHAPTER 1. GENERAL INTRODUCTION

Dissertation organization

This dissertation begins with a general introduction of topics related to this work. The following chapters contain three scientific manuscripts, each presented in a separate chapter with accompanying tables, figures, and literature citations. The final chapter summarizes the work and provides some prospective on this work.

This introduction starts with a brief treatment of the basic principles of electrophoresis separation, followed by a discussion of gel electrophoresis and particularly polyacrylamide gel electrophoresis for protein separation, a summary of common capillary electrophoresis separation modes, and a brief treatment of micro-bioanalysis application of capillary electrophoresis, and ends with an overview of protein conformation and dynamics.

Basic principles of electrophoresis

Electrophoresis refers to the migration of charged species under an external electric field. Complementary to various chromatography methods, electrophoresis is widely used as a high resolution separation technique for the separation and analysis of complex mixtures.

Under an external electric field E, a charged particle experiences a force F_e proportional to its net charge Q.

$$F_e = QE$$

If the particle moves under this external electric field, it experiences a drag force F_d that is proportional to its velocity, v, under non-turbulence conditions.

$$F_d = fv$$

where f is the translational friction coefficient.

Thus the electrophoretic mobility of a particle, μ, defined as the velocity per unit field strength under steady state, takes the form of

$$\mu = \frac{Q}{f}$$

In the simple case of a rigid spherical particle in free solution, the translational friction coefficient is given by:

$$f = 6\pi\eta r$$

where r is the radius of the particle and η is the viscosity of the media.

Particles with different charge to size ratio in free solution have different electrophoretic mobility and thus can be separated by electrophoresis.

Gels are assumed to be a random network of interconnected pores with an average pore size ξ. The electrophoretic mobility of a rigid spherical particle within a gel is given by the Ogston model[1]

$$\mu = \mu_0 P(\xi \geq r)$$

where μ_0 is the particle's electrophoretic mobility in free solution, $P(\xi \geq r)$ is the probability that a given pore has a radius greater than or equal to the radius of the particle (radius

r). Gel media thus superimpose a sieving, or filtration, effect on electrophoresis separation. Non-porous matrices or matrices with pores much larger than the electrophoresis species act only as an anti-convective support and provide no sieving selectivity.

For large molecules such as DNA, electrophoretic migration can still occur even when $r \ll \xi$ as they deform and "snake" through the interconnected pores like a reptile[2]. Assuming the solute behaves as a random coil, the translational friction coefficient, f_{rep}, for molecules undergoing this reptile motion is proportional to the square of the length or base pair number N of the DNA molecule.

$$f_{rep} \sim N^2$$

Since the charge of a DNA molecule is proportional to its base pair number,

$$Q \sim N$$

Thus reptile DNA mobility is inversely proportional to its size N

$$\mu \sim \frac{N}{N^2} = \frac{1}{N}$$

This means DNA separation in gel electrophoresis is primarily size based. The same is true for denatured protein with uniform charge as in the case of sodium dodecyl sulfate (SDS)-protein complex.

Additional effect of external electric field can deform the random coil, stretching the molecule along the direction of the field. A biased reptation model was described by Lumpkin et al[3].

$$\mu \approx \left(\frac{1}{N} + bE^2\right)$$

where *b* is a function of the gel's pore size and migrating molecule's charge and segment length. As the electrical field or the molecular size increases, the relative dependence of mobility on molecular size decreases. This in turn puts a practical upper size limit for DNA and SDS-protein separation by gel electrophoresis.

Gel electrophoresis

Although rapid development and application of electrophoresis only happened in the last three decades or so, the history of electrophoresis as a separation tool dates back to 1937 when Tiselius showed the electrophoretic separation of blood plasma proteins[4]. One intrinsic limitation on the resolution of electrophoresis separation, namely band broadening caused by Joule heating, was identified and only partially resolved by cooling with 4°C water in Tiselius' original work. The development of electrophoresis into a high resolution technique has largely been associated with the success in minimizing the detrimental effect of Joule heating. The strategy of using anti-convective matrix has led to the development of gel electrophoresis.

Filter paper was the first anti-convective supporting media[5] for electrophoresis and had great popularity in the 1940s and 1950s. The high content of carboxyls in filter paper, however, produces severe streaking due to additional chromatographic interaction[6]. Gordon et al.[7] introduced agar gel electrophoresis in 1950. One major component of agar, agaropectin, is highly charged with sulfate and carboxyl groups, producing strong electroendosmosis and sometimes adsorption of proteins[8] and gradually faded out of use; the other major component, agarose, is

almost neutral and still widely used in DNA and large protein separation today[9-11]. In 1955, Smithies[12] discovered the excellent resolving power of starch gel. Whereas cellulose used in paper is a linear polymer (300-2500 glucose units connected by 1, 4-β links), starch is made of two types of components: the linear amylose (~300 glucose units joined by 1, 4-α links) and the branched amylopectin (same structure as amylose, but branched through 1, 6-α links). Highly concentrated starch (14-15%) produces pores small enough to give sufficient frictional resistance to produce a sieving effect in the electrophoresis separation of macromolecules. This sieving effect, although only understood slowly, later became a unique feature, one with indispensible application, of gel electrophoresis.

Sieving as an electrophoresis separation mode was not fully realized until polyacrylamide[13] gel was used. The advantage of using polyacrylamide for sieving separation lies primarily in its great versatility in producing a range of pore sizes by varying the monomer to cross-linker ratio[14]. These pore sizes can be generated reproducibly due to its synthetic nature. This, together with lower fixed charge, better pH and chemical stability, and better mechanical strength[15] compared to its predecessors, has largely made polyacrylamide gel electrophoresis (PAGE) one of the most popular techniques for separation of large biomolecules, such as proteins, in virtually every biochemistry laboratory[16].

Polyacrylamide gel electrophoresis of proteins

The separation of protein mixtures from biological sources is an inherent task required for the detailed understanding of biology at the molecular level. The complexity of proteins from cells demands high resolution separation techniques such as ultracentrifugation and various

liquid chromatography and electrophoresis techniques[17]. Among them, polyacrylamide gel electrophoresis, or PAGE, is noticeably the most often used. The two most common modes of PAGE, isoelectric focusing (IEF) and SDS-PAGE, as well as the combination of the two, rely on the unique properties of the polyacrylamide gel.

Polyacrylamide gel

In electrophoresis, polyacrylamide refers to cross-linked polymer of acrylamide, which is a solid; the non-cross-linked polymer is commonly referred to as linear polyacrylamide, which is a viscous fluid. While both types can be used as anti-convective or sieving matrices and both are used in capillary gel electrophoresis, only the cross-linked gel can physically support the separation and hence is exclusively used in classic gel electrophoresis.

The great success of polyacrylamide is due mainly to its ability to produce various pore sizes by varying the starting monomer and cross-linker concentrations. Pore sizes are estimated to range from 0.5 to 500nm[18-21], depending upon matrix composition. Generally, smaller pore size is produced with higher concentration of monomer or higher percentage of cross-linker. For example, a total of 10.5% monomer containing 5% cross-linker gives a pore radius of about 21nm, whereas a total of 4.6% monomer containing 2% cross-linker produces a pore radius of about 200nm[21]. One can adjust the composition to produce gels as pure anti-convective support or as a sieving matrix as well.

Isoelectric focusing

Isoelectric focusing refers to the electrophoretic separation of amphoteric species in a pH gradient. Under an electric field and a parallel pH gradient, an amphoteric compound such as a protein will move to a region with a pH value equal to its isoelectric point (pI) where it has zero

net charge. Further moving up or down the pH gradient, the protein will acquire additional negative or positive charge and electrophoretically migrate back to its pI. IEF is a high resolution separation technique in that band broadening caused by diffusion is countered by electrophoretic focusing to give a steady state separation.

To achieve true steady state separation, a pH gradient stable under electric field is required. Early pH gradients were established by carrier ampholytes, which are a mixture of soluble amphoteric buffers with very close pI distribution and great buffer capacity at their pIs[22-24]. Carrier ampholytes were essential to the development of IEF and are still being used today. However, synthesis of carrier ampholytes has reproducibility issue and the pH gradient can drift over time[25]. Bjellqvist et al.[26] invented immobilized pH gradient (IPG) by incorporating acidic and basic derivatives of acrylamide gradient into polyacrylamide matrix during polymerization. The ampholytes are thus covalently affixed to the polyacrylamide matrix, greatly improving the stability of the pH gradient. Today, IPG is the stand medium for IEF separation[27].

In IEF, polyacrylamide serves as anti-convective, supporting matrix, and the sieving effect is minimized by using low concentration/large pore gels.

SDS- polyacrylamide gel electrophoresis

SDS-PAGE uses polyacrylamide as sieving matrix to separate SDS-bound proteins by their molecular weights (MW). Most proteins bind to SDS to a ratio of 1.4mg SDS/mg protein[28]. The large amount of negatively charged SDS masks the native charges of protein and gives the SDS-protein complex a constant charge-to-mass ratio. Under sieving condition, the electrophoretic mobility of SDS-protein is inversely proportional to its size, and linear

relationship between the logarithm of the MW and the relative migration distance can be established.

Polyacrylamide is the ideal matrix because of its great versatility in providing various pore sizes for protein mixtures of different size range. Furthermore, larger molecular range can be accommodated by using a porosity gradient gel generated through gradually increasing the gel percentage down the development direction of the separaion[29]. Also, stacking effect of a discontinuous gel concentration and buffer system can be employed to increase the resolution[30].

Two-dimensional polyacrylamide gel electrophoresis

Two-dimensional polyacrylamide gel electrophoresis (2D PAGE) combines the separation power of IEF and SDS-PAGE to separate proteins first on a strip gel by IEF and then further separates them on a slab gel by SDS-PAGE. Since IEF and SDS-PAGE are orthogonal, i.e. they separate proteins by totally different physical properties – the former by protein pIs and the latter by protein MWs, 2D PAGE can resolve thousands of protein on a single slab gel[31].

Although 2D PAGE is capable of high resolution, routine analysis with 2D PAGE is not a trivial task. In O'Farrell's original 2D PAGE work[31], in vivo ^{14}C- or ^{35}S-labeled proteins were separated first by IEF with a cylindrical gel cast inside a 130mm long, 2.5mm I.D. glass tube. After IEF, the gel had to be extruded with a 5mL syringe connected to the glass tube via a piece of Tygon tubing. Then the gel had to be shaken in SDS sample buffer to fully denature proteins and allow protein-SDS binding. The equilibrated cylindrical gel was laid parallel in front of the slab gel and fixed in place by pouring melted agarose gel, which solidifies after cooling to room temperature. Slab gels were dried after separation and detected by autoradiography.

Tremendous development in 2D PAGE has greatly simplified its operation since then[32]. Specialized instruments are used for each separation stage; pre-cast gels are now commercially available; IEF gels come in the form of dried strips with a plastic backing to facilitate handing; radioactive labeling detection has been largely replaced by fast staining and fluorescence-labeling methods; even robotics are used to achieve somewhat semi-automation. Yet the lack of full automation significantly hinders 2D PAGE's application in the ever increasing demand for throughput in proteome research[33-36].

The bottleneck to the full automation of 2D PAGE is the need to transfer the fragile gels. First, the orthogonal nature of IEF and SDS-PAGE requires two different gels and buffer systems. To ensure no interference, IEF is first carried out on a separate stage and the gel strip is then equilibrated with SDS buffer before laid on top of the slab gel for SDS-PAGE. Although transfer of IEF gel strip has been greatly simplified by bonding it covalently to a plastic backing, the dexterity of human hands is still indispensible.

Second, to visualize separated protein spots, staining or fluorescence labeling is generally required. However, the slab gel is commonly sandwiched between a pair of glass plates to increase the gel's strength and to facilitate heat-dissipation during SDS-PAGE. Dissembling the sandwich and transferring slab gels from solution to solution are delicate operations that require great care and skill. Similar to the IEF gel strips, slab gels backed on a plastic film are now available from commercial sources such as GE Health Care.

Covalent labeling of proteins prior to separation can potentially eliminate gel handling in the detection step. Existing pre-electrophoresis labeling methods inevitably modify the pI, size, or both of the proteins[37], leading to change of migration pattern[38]. More importantly,

derivatization is never complete, resulting in duplicated spots or streaking[39]. Protein solubility, especially with amino group modifying approaches, can be substantially reduced by labeling[40]. Co-electrophoretic staining by including non-covalent dyes, such as SYRPO Orange or SYPRO Red, in the running buffer of SDS-PAGE[41] also can greatly simplify detection. However, a destaining operation is required.

Label-free detection of proteins in polyacrylamide gel

Detection without labeling would potentially eliminate gel transfer and is ideal for automation.

Although mainly used for protein identification and characterization, mass spectrometry (MS) can also be used in label-free gel protein detection. As early as 1989, fast atom bombardment MS was used for detecting peptides[42] in polyacrylamide gel. Most attempts of direct MS detection of gel proteins use matrix-assisted desorption/ionization (MALDI) for better sensitivity. To make proteins accessible to the probing laser beam, gel proteins are often electroblotted to the surface of a polymeric membrane[43, 44]. More recently, direct sampling from ultra-thin gels of 10μm or less with matrix-assisted laser desorption/ionization mass spectrometry[45] had shown great sensitivity. The great advantage of direct MS detection is that protein can be simultaneously identified if necessary. However, all these current MS-based detection still requires gel manipulation, which is not amenable for automation.

Proteins are naturally UV absorptive and fluorescent. The peptide bond absorption peak around 214nm, however, is not useful here due to the strong absorption of polyacrylamide gel at this wavelength. The strong absorption of aromatic amino acids around 280nm offers better contrast to the polyacrylamide background, making direct UV detection possible. The sensitivity

is only in the microgram range[46, 47], which is comparable to the sensitivity of the commonly used coomassie blue dye stain[48]. Alternatively, native fluorescence of aromatic amino acids can be exploited[47, 49, 50] for gel protein detection with a detection limit comparable to or better than the nanogram range of silver stain[48]. Recently, Zhang et al.[51] improved the sensitivity of protein native fluorescence detection to picogram range by using laser side-entry excitation. More excitingly, native fluorescence detection can be employed *in situ* with no need for further gel manipulation.

A 2D PAGE separation and detection platform amenable to full automation is described in the second chapter.

Capillary Electrophoresis

Rather than using a solid anti-convective matrix, Hjerten[52] in 1967 realized that running electrophoresis in a narrow bore tube can effectively reduce the band broadening effect of Joule heating. Due to technical limitation in glass drawing, Hjerten's original 3mm inner diameter (ID), 7.6mm outer diameter (OD) quartz tube, although permitting "free zone electrophoresis" in the absence of a supporting metrix, was not very efficient in heat dissipation. Smaller diameter tubes such as 250-500μm Pyrex glass[53] and 200μm Teflon[54] were also used later. But electrophoresis in a tube did not gain much attention until 1981 when Jorgenson and Lukacs[55] demonstrated the high resolving power of free solution electrophoresis inside a 75μm ID glass capillary. The high surface-to-volume ratio capillary provided effective heat dissipation and thus allowed electric field as high as 300V/cm to be applied for fast and high efficient separation.

Since 1981, tremendous new advances have now broadened the term “capillary electrophoresis” to encompass a family of specialized separation techniques using electric field and capillary channels. Common modes of CE include capillary zone electrophoresis (CZE), capillary gel electrophoresis (CGE), capillary isoelectric focusing (CIEF), micellar electrokinetic chromatography (MEKC), and capillary electrochromatography (CEC). Comparing to slab gel electrophoresis, CE generally offers higher separation efficiency, shorter analysis time, lower sample consumption, and full automation.

CZE is the basic mode of CE separation. Analyte ions are separated into discrete zones as a result of their unequal mobilities in free solution. Fine-tuning of CZE separation is achieved by changing buffer (buffer composition, ionic strength, pH, etc.), capillary (dimension, surface chemistry), and operating parameters (electric field and temperature). CZE has been successfully applied in separation of both inorganic ions[56-59] and organic ions such as small organic ions[60, 61], peptides[62-64], proteins[65-67], carbohydrates[68, 69], and nucleic acids[70, 71]. Various chiral discriminating agents[72-75] such as cyclodextrins[76] have been used in CZE buffer to perform chiral separation.

CGE is gel electrophoresis run in a capillary. Like its slab format counterpart, CGE is primarily used for separation of biopolymers[77] such as nucleic acids[78, 79], proteins[80], and carbohydrates[81]. Unlike slab gel electrophoresis, CGE use gels only as sieving media. Since the supportive role is taken by the capillary, solid gels are not required in CGE. Fluidic polymer solutions that can effectively produce the appropriate pore sizes can be used. Commonly used polymers for CGE include linear polyacrylamide and its derivatives[82, 83], cellulose and its derivatives[84], polyvinyl alcohol[85], poly(ethylene oxide)[86], and polyvinylpyrrolidone[87]. These fluidic gels can be easily replaced without sacrificing the capillary. CGE separation can be

optimized by changing gel composition in addition to other variables available in CZE. It is very interesting to note that CGE, the hybrid of GE and CE, later became the analytical tool that helped to produce one of the greatest achievements of the 20th century in that it provided the vast majority of the sequence information for the Human Genome Project[88].

IEF in capillary was first carried out by Hjerten and Zhu[89] in 1985. Besides using free solution in a capillary, CIEF is also different from conventional gel IEF in terms of detection methods. Whereas slab gel matrices are usually imaged off-line with a scanner or a 2D array detector, CE detection is usually on-line with a point detector fixed downstream along the capillary. Consequently, CIEF detection requires either the whole pH gradient to be mobilized or some modification in the detection scheme. Commonly used pH gradient mobilization methods include hydrodynamic mobilization[90], salt mobilization[91], and simultaneous focusing and mobilization[92]. Special detection schemes such as capillary scanning[93] and whole-column array detection[94] have also been used.

CEC and MEKC are hybrids of CE and liquid chromatography (LC). Introduced by Jorgenson and Lukacs in 1981[95], CEC is essentially LC without a pump. Solvent flow in CEC is driven by electroosmotic flow (EOF) rather than hydraulic pressure. EOF arises in the electrical double layer at the solid-liquid interface. The main advantages of using EOF for chromatographic separations are its plug flow profile and the ability to use much smaller stationary phase particles – the plug flow profile minimizes eddy effect; smaller stationary phase particles reduce dispersion caused by mass transfer – both significant in improving LC efficiency. Column efficiency of 150,000 to 200,000 plates/meter were demonstrated by Erni et al.[96] with 50μm ID capillaries packed with 3μm diameter ODS-Hypersil particles.

MEKC was unveiled by Terabe et al.[97] in 1984 by adding surfactant SDS in the running buffer with a concentration above the critical micelle concentration (CMC). These micelles provide a secondary phase, so called "pseudostationary", other than the running buffer. Chromatographic partitioning of analytes between buffer solution and micelles was superimposed into normal electrophoresis separation. Similar to CEC, the plug flow profile EOF and small secondary phase particle – in this case, colloidal-size micelles – enable high efficiency chromatographic separation. Comparing to traditional LC, MEKC is also more versatile in terms of using a variety of micellar pseudostationary phase[98] to provide different selectivity.

The chromatographic nature of CEC and MEKC enables CE to be applied to the separation of neutral species as well as ions. In practice, CEC and MEKC are generally performed with aqueous buffer in order to utilize the strong EOF, hence separate with reverse phase rather than normal phase LC.

Micro-bioanalysis with capillary electrophoresis

CE is not just a separation technique. The small volume (e.g. 314pL/mm of a 20μm ID capillary) makes capillary a natural nano-sampler and nano-reactor. In many instances, the limited availability of biological sample significantly hinders the analysis. This is particularly true when analysis has to be targeted at a group of cells, single cells, or even at single molecules. Off-line preparation of nanoliter or less sample using a relatively large (milliliter to microliter) reaction or manipulation volume is at least not effective if not futile. The combination of high efficiency separation and small sampling/reaction volume has found CE a great deal of

application in bio-fluid analysis[99], DNA sequencing[100], peptide mass finger-printing[101], immune assay[102, 103], enzyme assay[104], and single cell analysis[105].

Single cell analysis with CE

Single cell analysis with CE usually involves injecting a single cell into the capillary, lysing the cell via chemical, electrical, or optical methods inside the capillary, and separating and detecting the lystate's contents by sensitive detection techniques such as laser induced fluorescence, electrochemical detection, and mass spectrometry. Various cell contents have been analyzed at single cell level with CE. To name just a few examples, proteins from single erythrocytes were first analyzed inside a 20μm capillary by Lee and Yeung[106]; Dovichi's group recently developed two-dimensional separation combining CGE and MEKC to study the proteome of single mammalian cells[107]; neurotransmitter catecholamines were identified to be present in human lymphocytes[108] by single cell CE; nitric oxide-related metabolites in single neurons were studied by Sweedler's group[109]; single-cell genotyping was performed by Li and Yeung[110] for human lymphoblast cells.

The third chapter of thesis describes a CZE based method for determining the amount of an important redox pair, β-nicotinamide adenine dinucleotide (NAD^+) and its reduced form NADH, in single cells.

On-line enzyme assay with CE

Monitoring enzyme reaction is another great area of applications that couples on-line reaction with CE. Depending on the goal of the analysis, either heterogeneous enzyme reaction or homogeneous reaction in solution can be carried out in the electrophoresis capillary. In the heterogeneous approach, one of the reactants, usually the enzyme is immobilized on the surface

of a suitable section of the capillary to form a micro-reactor. Reaction products are directly transported and separated by CE. In homogeneous enzyme assay, all reactants, including the enzyme, are present in solution. Electrophoresis is the sole mediator of reactants mixing, separation, and detection. Whereas the objective of heterogeneous approach is primarily to determine substrates and inhibitors or to monitor reaction kinetics, the homogeneous method is mainly used to assay the enzyme activity.

Bao and Regnier[111] described the first homogeneous enzyme assay in capillary in 1992. Enzyme glucose-6-phosphate dehydrogenase (G-6-PDH) was injected to a capillary that contained substrate glucose-6-phosphate (G-6-P) and coenzyme oxidized nicotinamide adenine dinucleotide phosphate ($NADP^+$), and the product, reduced nicotinamide adenine dinucleotide phosphate (NADPH) was detected with UV absorption at 340nm. If a constant voltage was applied, products were formed and separated from the enzyme because of their difference in electrophoretic mobility. G-6-PDH thus swept through the substrates filled capillary, producing a plateau of NADPH that would go through the detector by electrophoretic transportation. If the voltage was switched off for a few minutes during the run, local accumulation of NADPH would occur where the enzyme was and later be detected as a peak on top of the plateau.

This homogeneous enzyme assay is later dubbed electrophoretically mediated microanalysis (EMMA)[112]. Additionally, this particular mode of operation, where the enzyme is in continuous contact with all the reactants during the analysis, is designated as “continuous mode EMMA”. In the other “plug-plug mode EMMA”, enzyme and substrates are injected as separate zones and only brought into contact by exploiting the difference in their electrophoretic mobilities. As an example, Kwak et al.[113] assayed the same G-6-PDH enzyme by first injecting a plug of the slower moving enzyme, and then injecting a plug of the faster moving NAD^+. The

enzyme caught up and surpassed the NAD^+ zone before reaching the detector. Since the other substrate G-6-P is present in the background, reaction occurred during the brief contact of the enzyme and NAD^+. Both the substrate NAD^+ and the product NADH were detected as isolated peaks.

Single enzyme molecule assay in capillary

A host of enzymes[114] have been assayed by EMMA. Of particular interest is the special application of EMMA in single enzyme molecule assay pioneered by Xue and Yeung[115]. In their original work, a 20μm capillary was filled with a buffer containing a very diluted lactate dehydrogenase (LDH) and substrate (lactate and NAD^+) and incubated for 1hr for products NADH to accumulate. Then the voltage was turned on to electrophoretically drive NADH products through the detector. Since the enzyme concentration is so low, on average, individual enzyme molecules are separated by several centimeters. The discrete NADH product pools from individual enzymes did not mix by diffusion during the relatively short incubation time. Thus NADH products were detected as isolated peaks whose areas were proportional to the corresponding enzyme molecule activity.

The most interesting aspect of this experiment is the finding that LDH molecules are not uniform in terms of their catalytic activities. Subsequent studies on alkaline phosphatase[116, 117] and β-galactosidase[118, 119] using similar method by Craig et al. found that this heterogeneity is not unique to LDH. While catalytic activity heterogeneity certainly reflects structural diversity, the exact nature of the structural diversity is not so obvious. Both conformational heterogeneity[115] and primary sequence heterogeneity[116] (results of post-translational modifications) were proposed.

Enzyme molecule conformation

Most enzymes are proteins. One unique feature of macromolecules such as proteins is their flexibility and the ability to have multiple conformations[120]. The conformations of all proteins are constantly fluctuating with a time scale ranging from picoseconds or less to milliseconds depending on the scale of conformation change[121-125]. The time scale is within the typical millisecond scale of enzyme catalytic cycle and thus conformational fluctuation has long been associated with enzyme catalysis ever since the "induced fit model" of enzyme-substrate binding was put forth by Koshland[126]. The fact that multiple intermediates are almost always detected for enzymes with established comprehensive mechanisms[120] is overwhelming evidence supporting coupling of conformational changes and enzyme catalysis. And there is increasing popularity for the idea that biology has channeled the inherent random conformational fluctuation of enzymes into productive events[127].

Protein conformers existing on the time scale comparable to an enzymatic cycle are also evident. Early experiments on dispersed kinetics of rebinding of carbon monoxide and oxygen ligands to myoglobin after photodissociation[128] and later spectral relaxation of the same system[129, 130] indicated conformers stable in time scale up to milliseconds. Single enzyme molecule catalysis reaction trajectory experiments show dynamic fluctuations of rate constant at a broad range of time scales (from 1 millisecond to 100 seconds) for cholesterol oxidase[131], horseradish peroxide[132], lipase[133], and λ-exonulcease[134]. A fluctuating enzyme model[131] where multiple enzymatic conformations interconvert on the time scale of catalytic activity was proposed to explain the observed dynamic of enzyme activity and supported by electron transfer[135-137], fluorescence resonance energy transfer[138, 139], and NMR[140] studies.

Conformations with a much longer lifetime were first detected in a gaseous phase by mass spectrometry[141]. For enzymes in solution, Xue's experiments[115] on two consecutive incubation of the same LDH molecule showed stable activity over 2 hours in room temperature. Similar experiments showed that alkaline phosphatase[116] and β-galactosidase[118] also give consistent time-averaged activity for 15 minutes incubation. Stable conformations on such time scale, however, have not been directly observed in solution.

Put back to its physiological conditions, a denatured protein undergoes a spontaneous transition from a random coil to its native, three-dimensional structure. The folding free energy landscape is believed to be funnel-shaped[121, 142]. However, the funnel surface is rugged at certain regions due to non-native interaction, resulting in local energy minima and multiple protein conformations. The spin glass model, originally introduced in the random magnetic system by Anderson[143], was imported to protein folding by Wolynes et al.[144] to illustrate the metastable conformations, or "frustrations", of protein *en route* to the spout of the energy funnel. The spin glass model dictates that a system with multiple discrete variables tends to interact in a random and conflicting way, very much like the hydrogen bonding and steric interaction in protein folding, making it difficult to determine the lowest energy configuration. A spin glass type energy landscape confers both stability due to local minima and diversity due to the existence of multiple minima. The rarity of experimental observation of long-lived conformers was taken as evolutional evidence[145] – amino acid sequence selected by nature to give minimal non-native interaction and a relatively smooth energy funnel surface.

Recent X-ray crystallography study on human lactate dehydrogenase isozyme 1 revealed multiple conformations of LDH from crystals obtained from the sample crystallization mother liquor. The active site loop of any of the four subunits can be in an open conformation, closed

conformation, or two conformations[146]. Since crystallization did not seem to cause differentiation of conformations, these multiple apparently stable conformations were believed to exist in solution. Chapter four presents an activity study on these crystals in an effort to investigate the origin of this conformational heterogeneity and its effect on enzyme activity.

References

(1) Ogston, A. G. *Trans. Faraday Soc.* **1958**, *54*, 1754.

(2) Lerman, L. S.; Frisch, H. L. *Biopolymers* **1982**, *21*, 995-997.

(3) Lumpkin, O. J.; Dejardin, P.; Zimm, B. H. *Biopolymers* **1985**, *24*, 1573-1593.

(4) Tiselius, A. *Trans. Faraday Soc.* **1937**, *33*, 524-531.

(5) von Klobusitzky, D.; Konig, P. *Naunyn-Schmiedebergs Archiv für Experimentelle Pathologie und Pharmakologie* **1939**, *192*, 271-275.

(6) Righetti, P. G. *J. Chromatogr., A* **2005**, *1079*, 24-40.

(7) Gordon, A. H.; Keil, B.; Sebesta, K.; Knessl, O.; Sorm, F. *Collect Czech Chem. C.* **1950**, *15*, 1-16.

(8) Wieme, R. J. *Agar gel electrophoresis*; Elsevier: Amsterdam 1965.

(9) Greenspan, P.; Mao, F. W.; Ryu, B. H.; Gutman, R. L. *J. Chromatogr., A* **1995**, *698*, 333-339.

(10) Borst, P. *IUBMB Life* **2005**, *57*, 745-747.

(11) Righetti, P. G. *Isoelectric focusing: Theory, methodology and applications*; Elsevier: New York, 1983.

(12) Smithies, O. *Biochem. J.* **1955**, *61*, 629-641.

(13) Raymond, S.; Weintraub, L. *Science (Washington, DC, U. S.)* **1959**, *130*, 711.

(14) Raymond, S. *Ann. NY. Acad. Sci* **1964**, *121*, 350-365.

(15) Hawcroft, D. M. *Electrophoresis*; Oxford University Press: New York 1997.

(16) Righetti, P. G.; Gelfi, C. In *Handbook of analytical techniques*; Gunzler, H., Williams, A., Eds.; Wiley-VCH: New York, 2001.

(17) Janson, J.-C.; Ryden, L. *Protein purification: Principles, high-resolution methods, and applications*; Wiley-VCH: New York, 1998.

(18) Righetti, P. G.; Caglio, S.; Saracchi, M.; Quaroni, S. *Electrophoresis* **1992**, *13*, 587-595.

(19) Diana L. Holmes, N. C. S. *Electrophoresis* **1991**, *12*, 612-619.

(20) Ruechel, R.; Steere, R. L.; Erbe, E. F. *J. Chromatogr.* **1978**, *166*, 563-575.

(21) Stellwagen, N. C. *Electrophoresis* **1998**, *19*, 1542-1547.

(22) Svensson, H. *Acta Chem. Scand.* **1961**, *15*, 325-341.

(23) Svensson, H. *Acta Chem. Scand.* **1962**, *16*, 456-466.

(24) Vesterberg, O. *Acta Chem. Scand.* **1969**, *23*, 2653-2666.

(25) Hjerten, S. In *Capillary electrophoresis: theory and practice*; Grossman, P. D., Colburn, J. C., Eds.; Academic Press: San Diego, 1992.

(26) Bjellqvist, B.; Ek, K.; Giorgio Righetti, P.; Gianazza, E.; Gorg, A.; Westermeier, R.; Postel, W. *J. Biochem. Biophys. Methods* **1982**, *6*, 317-339.

(27) Gorg, A.; Obermaier, C.; Boguth, G.; Harder, A.; Scheibe, B.; Wildgruber, R.; Weiss, W. *Electrophoresis* **2000**, *21*, 1037-1053.

(28) Pittrive, R.; Impiomba, F. *Biochem. J.* **1968**, *109*, 825-831.

(29) Margolis, J.; Kenrick, K. G. *Anal. Biochem.* **1968**, *25*, 347-355.

(30) Laemmli, U. K. *Nature (London, U. K.)* **1970**, *227*, 680-681.

(31) O'Farrell, P. H. *J. Biol. Chem.* **1975**, *250*, 4007-4021.

(32) Quadroni, M.; James, P. *Electrophoresis* **1999**, *20*, 664-677.

(33) Garbis, S.; Lubec, G.; Fountoulakis, M. *J. Chromatogr., A* **2005**, *1077*, 1-18.

(34) Fey, S. J.; Larsen, P. M. *Curr. Opin. Chem. Biol.* **2001**, *5*, 26-33.

(35) Van den Bergh, G.; Arckens, L. *Expert Rev. Proteomics* **2005**, *2*, 243-252.

(36) Hiratsuka, A.; Kinoshita, H.; Maruo, Y.; Takahashi, K.; Akutsu, S.; Hayashida, C.; Sakairi, K.; Usui, K.; Shiseki, K.; Inamochi, H.; Nakada, Y.; Yodoya, K.; Namatame, I.; Unuma, Y.; Nakamura, M.; Ueyama, K.; Ishii, Y.; Yano, K.; Yokoyama, K. *Anal. Chem.* **2007**, *79*, 5730-5739.

(37) Wayne, F. P. *Electrophoresis* **2000**, *21*, 1123-1144.

(38) de Jong, W. W.; Zweers, A.; Cohen, L. H. *Biochem. Biophys. Res. Commun.* **1978**, *82*, 532-539.

(39) Peter Jackson, V. E. U. C. D. M. *Electrophoresis* **1988**, *9*, 330-339.

(40) Marc R. Wilkins, E. G. J.-C. S. A. B. D. F. H. *Electrophoresis* **1998**, *19*, 1501-1505.

(41) Steinberg, T. H.; Jones, L. J.; Haugland, R. P.; Singer, V. L. *Anal. Biochem.* **1996**, *239*, 223-237.

(42) Camilleri, P.; Haskins, N. J.; Hill, A. J.; New, A. P. *Rapid Commun. Mass Spectrom.* **1989**, *3*, 440-442.

(43) Strupat, K.; Karas, M.; Hillenkamp, F.; Eckerskorn, C.; Lottspeich, F. *Anal. Chem.* **1994**, *66*, 464-470.

(44) Vestling, M. M.; Fenselau, C. *Anal. Chem.* **1994**, *66*, 471-477.

(45) Ogorzalek Loo, R. R.; Stevenson, T. I.; Mitchell, C.; Loo, J. A.; Andrews, P. C. *Anal. Chem.* **1996**, *68*, 1910-1917.

(46) Yamamoto, H.; Nakatani, M.; Shinya, K.; Kim, B.-H.; Kakuno, T. *Anal. Biochem.* **1990**, *191*, 58-64.

(47) Koutny, L. B.; Yeung, E. S. *Anal. Chem.* **1993**, *65*, 183-187.

(48) Rabilloud, T. *Proteome research: Two-dimensional gel electrophoresis and identification methods*; Springer-Verlag: Berlin, 2000.

(49) Roegener, J.; Lutter, P.; Reinhardt, R.; Bluggel, M.; Meyer, H. E.; Anselmetti, D. *Anal. Chem.* **2003**, *75*, 157-159.

(50) Sluszny, C.; Yeung, E. S. *Anal. Chem.* **2004**, *76*, 1359-1365.

(51) Zhang, H.; Yeung, E. S. *Electrophoresis* **2006**, *27*, 3609-3618.

(52) Hjerten, S. *Chromatogr. Rev.* **1967**, *9*, 122-219.

(53) Virtanen, R. *Acta Polytech. Sc. Ch.* **1974**, *123*, 67.

(54) Mikkers, F. E. P.; Everaerts, F. M.; Verheggen, T. P. E. M. *J. Chromatogr.* **1979**, *169*, 11-20.

(55) Jorgenson, J. W.; Lukacs, K. D. *Anal. Chem.* **1981**, *53*, 1298-1302.

(56) Timerbaev, A. R. *Talanta* **2000**, *52*, 573-606.

(57) Timerbaev, A. R. *Electrophoresis* **2002**, *23*, 3884-3906.

(58) Timerbaev, A. R. *Electrophoresis* **2004**, *25*, 4008-4031.

(59) Timerbaev, A. R. *Electrophoresis* **2007**, *28*, 3420-3435.

(60) Fritz, J. S. *J. Chromatogr., A* **2000**, *884*, 261-275.

(61) Chen, R.; Cheng, H.; Wu, W.; Ai, X.; Huang, W.; Wang, Z.; Cheng, J. *Electrophoresis* **2007**, *28*, 3347-3361.

(62) Messana, I.; Rossetti, D. V.; Cassiano, L.; Misiti, F.; Giardina, B.; Castagnola, M. *J. Chromatogr., B: Anal. Technol. Biomed. Life Sci.* **1997**, *699*, 149-171.

(63) Lee, H. G.; Desiderio, D. M. *Anal. Chim. Acta* **1999**, *383*, 79-99.

(64) Trujillo, A. J.; Pavia, M.; Ferragut, V.; Casals, I.; Guamis, B. *Recent Res. Dev. Agric. Food Chem.* **2000**, *4*, 239-255.

(65) Dolnik, V. *Electrophoresis* **1997**, *18*, 2353-2361.

(66) Dolnik, V. *Electrophoresis* **1999**, *20*, 3106-3115.

(67) Hempe, J. M. In *Handbook of capillary and microchip electrophoresis and associated microtechniques,* 3rd ed.; Landers, J. P., Ed.; CRC: Boca Raton, 2007.

(68) Oefner, P. J.; Chiesa, C. *Glycobiology* **1994**, *4*, 397-412.

(69) Zhang, J.-B.; Tain, G.-Y. *Youji Huaxue* **1998**, *18*, 88-96.

(70) Huang, M.; Liu, S.; Murray, B. K.; Lee, M. L. *Anal. Biochem.* **1992**, *207*, 231-235.

(71) Righetti, P. G.; Gelfi, C.; Perego, M.; Stoyanov, A. V.; Bossi, A. *Electrophoresis* **1997**, *18*, 2145-2153.

(72) Guebitz, G.; Schmid, M. G. *Electrophoresis* **2007**, *28*, 114-126.

(73) Vespalec, R.; Bocek, P. *Electrophoresis* **1999**, *20*, 2579-2591.

(74) Vespalec, R.; Bocek, P. *Electrophoresis* **1997**, *18*, 843-852.

(75) Zhong, Y.; Zhu, X.; Xu, X.; Lin, B. *Fenxi Huaxue* **1999**, *27*, 719-725.

(76) Koppenhoefer, B.; Zhu, X.; Jakob, A.; Wuerthner, S.; Lin, B. *J. Chromatogr., A* **2000**, *875*, 135-161.

(77) Guttman, A. *J. Chromatogr. Sci.* **2003**, *41*, 449-459.

(78) Mitchelson, K. R.; Cheng, J. *Capillary electrophoresis of nucleic acids, volume 1: Introduction to the capillary electrophoresis of nucleic acids*; Humana press: Totowa, 2001.

(79) Mitchelson, K. R.; Cheng, J. *Capillary electrophoresis of nucleic acids, volume II: Practical applications of capillary electrophoresis* Humana Press: Totowa, 2001.

(80) Guttman, A. *Electrophoresis* **1996**, *17*, 1333-1341.

(81) Guttman, A. *Nature (London, U. K.)* **1996**, *380*, 461-462.

(82) Ruiz-Martinez, M. C.; Berka, J.; Belenkii, A.; Foret, F.; Miller, A. W.; Karger, B. L. *Anal. Chem.* **1993**, *65*, 2851-2858.

(83) Carrilho, E.; Ruiz-Martinez, M. C.; Berka, J.; Smirnov, I.; Goetzinger, W.; Miller, A. W.; Brady, D.; Karger, B. L. *Anal. Chem.* **1996**, *68*, 3305-3313.

(84) Bashkin, J.; Marsh, M.; Barker, D.; Johnston, R. *Appl. Theor. Electroph.* **1996**, *6*, 23-28.

(85) Simo-Alfonso, E.; Conti, M.; Gelfi, C.; Righetti, P. G. *J. Chromatogr., A* **1995**, *689*, 85-96.

(86) Chang, H.-T.; Yeung, E. S. *J. Chromatogr., B: Anal. Technol. Biomed. Life Sci.* **1995**, *669*, 113-123.

(87) Gao, Q.; Yeung, E. S. *Anal. Chem.* **1998**, *70*, 1382-1388.

(88) Dovichi, N. J.; Zhang, J. *Angew. Chem., Int. Ed.* **2000**, *39*, 4463-4468.

(89) Hjerten, S.; Zhu, M. D. *J. Chromatogr., A* **1985**, *346*, 265-270.

(90) Hjertén, S. *J. Chromatogr., A* **1985**, *347*, 191-198.

(91) Hjertén, S.; Liao, J.-L.; Yao, K. *J. Chromatogr., A* **1987**, *387*, 127-138.

(92) Mazzeo, J. R.; Krull, I. S. *Anal. Chem.* **1991**, *63*, 2852-2857.

(93) Wang, T.; Hartwick, R. A. *Anal. Chem.* **1992**, *64*, 1745-1747.

(94) Thormann, W.; Tsai, A.; Michaud, J.-P.; Mosher, R. A.; Bier, M. *J. Chromatogr., A* **1987**, *389*, 75-86.

(95) Jorgenson, J. W.; Lukacs, K. D. *J. Chromatogr.* **1981**, *218*, 209-216.

(96) Yamamoto, H.; Baumann, J.; Erni, F. *J. Chromatogr., A* **1992**, *593*, 313-319.

(97) Terabe, S.; Otsuka, K.; Ichikawa, K.; Tsuchiya, A.; Ando, T. *Anal. Chem.* **1984**, *56*, 111-113.

(98) Terabe, S. *Anal. Chem.* **2004**, *76*, 241A-246A.

(99) Bergquist, J.; Gilman, S. D.; Ewing, A. G.; Ekman, R. *Anal. Chem.* **1994**, *66*, 3512-3518.

(100) Xue, G.; Pang, H. M.; Yeung, E. S. *J. Chromatogr., A* **2001**, *914*, 245-256.

(101) Chang, H. T.; Yeung, E. S. *Anal. Chem.* **1993**, *65*, 2947-2951.

(102) Ma, Y.; Shortreed, M. R.; Li, H.; Huang, W.; Yeung, E. S. *Electrophoresis* **2001**, *22*, 421-426.

(103) Yang, W.-C.; Yeung, E. S.; Schmerr, M. J. *Electrophoresis* **2005**, *26*, 1751-1759.

(104) Novakova, S.; Van Dyck, S.; Van Schepdael, A.; Hoogmartens, J.; Glatz, Z. *J. Chromatogr., A* **2004**, *1032*, 173-184.

(105) Huang, W.-H.; Ai, F.; Wang, Z.-L.; Cheng, J.-K. *J. Chromatogr., B: Anal. Technol. Biomed. Life Sci.* **2008**, *866*, 104-122.

(106) Lee, T. T.; Yeung, E. S. *Anal. Chem.* **1992**, *64*, 3045-3051.

(107) Hu, S.; Michels, D. A.; Fazal, M. A.; Ratisoontorn, C.; Cunningham, M. L.; Dovichi, N. J. *Anal. Chem.* **2004**, *76*, 4044-4049.

(108) Bergquist, J.; Tarkowski, A.; Ekman, R.; Ewing, A. *Proc. Natl. Acad. Sci. U. S. A.* **1994**, *91*, 12912-12916.

(109) Moroz, L. L.; Dahlgren, R. L.; Boudko, D.; Sweedler, J. V.; Lovell, P. *J. Inorg. Biochem.* **2005**, *99*, 929-939.

(110) Li, H.; Yeung, E. S. *Electrophoresis* **2002**, *23*, 3372-3380.

(111) Bao, J.; Regnier, F. E. *J. Chromatogr., A* **1992**, *608*, 217-224.

(112) Regnier, F. E.; Patterson, D. H.; Harmon, B. J. *Trac-Trend. Anal. Chem.* **1995**, *14*, 177-181.

(113) Kwak, E. S.; Esquivel, S.; Gomez, F. A. *Anal. Chim. Acta* **1999**, *397*, 183-190.

(114) Glatz, Z. *J. Chromatogr., B: Anal. Technol. Biomed. Life Sci.* **2006**, *841*, 23-37.

(115) Xue, Q.; Yeung, E. S. *Nature (London, U. K.)* **1995**, *373*, 681-683.

(116) Craig, D. B.; Arriaga, E.; Wong, J. C. Y.; Lu, H.; Dovichi, N. J. *J. Am. Chem. Soc.* **1996**, *118*, 5245-5253.

(117) Ashley C. Dyck, D. B. C. *Luminescence* **2002**, *17*, 15-18.

(118) Nichols, E. R.; Gavina, J. M. A.; McLeod, R. G.; Craig, D. B. *Protein J.* **2007**, *26*, 95-105.

(119) Shoemaker, G. K.; Juers, D. H.; Coombs, J. M. L.; Matthews, B. W.; Craig, D. B. *Biochemistry* **2003**, *42*, 1707-1710.

(120) Hammes, G. G. *Biochemistry* **2002**, *41*, 8221-8228.

(121) Frauenfelder, H.; Sligar, S. G.; Wolynes, P. G. *Science (Washington, DC, U. S.)* **1991**, *254*, 1598-1603.

(122) Karplus, M.; McCammon, J. A. *Nat. Struct. Mol. Biol.* **2002**, *9*, 646-652.

(123) Krishna, M. M. G.; Hoang, L.; Lin, Y.; Englander, S. W. *Methods* **2004**, *34*, 51-64.

(124) Mittermaier, A.; Kay, L. E. *Science (Washington, DC, U. S.)* **2006**, *312*, 224-228.

(125) Lindorff-Larsen, K.; Best, R. B.; DePristo, M. A.; Dobson, C. M.; Vendruscolo, M. *Nature (London, U. K.)* **2005**, *433*, 128-132.

(126) Koshland, D. E. *Proc. Natl. Acad. Sci. U. S. A.* **1958**, *44*, 98-104.

(127) Boehr, D. D.; McElheny, D.; Dyson, H. J.; Wright, P. E. *Science (Washington, DC, U. S.)* **2006**, *313*, 1638-1642.

(128) Austin, R. H. B., K. W.; Eisenstein, L.; Frauenfelder, H.; Gunsalus, I. C. *Biochemistry* **1975**, *14*.

(129) Lim, M.; Jackson, T. A.; Anfinrud, P. A. *Proc. Natl. Acad. Sci. U. S. A.* **1993**, *90*, 4.

(130) Hagen, S. J.; Eaton, W. A. *J. Chem. Phys.* **1996**, *104*, 3395-3398.

(131) Lu, H. P.; Xun, L.; Xie, X. S. *Science (Washington, DC, U. S.)* **1998**, *282*, 1877-1882.

(132) Edman, L.; Foldes-Papp, Z.; Wennmalm, S.; Rigler, R. *Chem. Phys.* **1999**, *247*, 11-22.

(133) Velonia, K.; Flomenbom, O.; Loos, D.; Masuo, S.; Cotlet, M.; Engelborghs, Y.; Hofkens, J.; Rowan, A., E.; Klafter, J.; Nolte, R. J. M.; de Schryver, F. C. *Angew. Chem., Int. Ed.* **2005**, *44*, 560-564.

(134) van Oijen, A. M.; Blainey, P. C.; Crampton, D. J.; Richardson, C. C.; Ellenberger, T.; Xie, X. S. *Science (Washington, DC, U. S.)* **2003**, *301*, 1235-1238.

(135) Yang, H.; Luo, G.; Karnchanaphanurach, P.; Louie, T.-M.; Rech, I.; Cova, S.; Xun, L.; Xie, S. X. *Science (Washington, DC, U. S.)* **2003**, *302*, 262-266.

(136) Min, W.; Luo, G.; Cherayil, B. J.; Kou, S. C.; Xie, X. S. *Phys. Rev. Lett.* **2005**, *94*, 1983021-1983024.

(137) Li, C.-B.; Yang, H.; Komatsuzaki, T. *Proc. Natl. Acad. Sci. U. S. A.* **2008**, *105*, 536-541.

(138) Zhuang, X.; Kim, H.; Pereira, M. J. B.; Babcock, H. P.; Walter, N. G.; Chu, S. *Science (Washington, DC, U. S.)* **2002**, *296*, 1473-1476.

(139) Kuznetsova, S.; Zauner, G.; Aartsma, T. J.; Engelkamp, H.; Hatzakis, N.; Rowan, A. E.; Nolte, R. J. M.; Christianen, P. C. M.; Canters, G. W. *Proc. Natl. Acad. Sci. U. S. A.* **2008**, *105*, 3250-3255.

(140) Vallurupalli, P.; Kay, L. E. *Proc. Natl. Acad. Sci. U. S. A.* **2006**, *103*, 11910-11915.

(141) Suckau, D.; Shi, Y.; Beu, S. C.; Senko, M. W.; Quinn, J. P.; Wampler, F. M.; McLafferty, F. W. *Proc. Natl. Acad. Sci. U. S. A.* **1993**, *90*, 790-793.

(142) Bryngelson, J. D.; Onuchic, J. N.; Socci, N. D.; Wolynes, P. G. *Proteins: Struct., Funct., Bioinf.* **1995**, *21*, 167-195.

(143) Kotliar, G.; Anderson, P. W.; Stein, D. L. *Phys. Rev. B: Condens. Matter Mater. Phys.* **1983**, *27*, 602-605.

(144) Bryngelson, J. D.; Wolynes, P. G. *Proc. Natl. Acad. Sci. U. S. A.* **1987**, *84*, 7524-7528.

(145) Rose, G. D.; Fleming, P. J.; Banavar, J. R.; Maritan, A. *Proc. Natl. Acad. Sci. U. S. A.* **2006**, *103*, 16623-16633.

(146) Li, F. Ph.D., Iowa State University, Ames, Iowa, 2006.

CHAPTER 2. PROTOTYPE FOR INTEGRATED TWO-DIMENSIONAL GEL ELECTROPHORESIS FOR PROTEIN SEPARATION

A paper published in Journal of Chromatography A*

Aoshuang Xu, Chanan Sluszny and Edward S. Yeung

Abstract

Two-dimensional gel electrophoresis practitioners have long waited for a fully automated system. This article presents an integrated platform that is capable of complete automation from sample introduction to spots detection. The strip gel for the first dimensional separation is fixed on the edge of a discrete planar stage before separation. A pair of platinum pin electrodes for isoelectric focusing (IEF) makes contact from underneath the stage. IEF is performed directly after rehydration and protein loading. After the first dimensional separation, sodium dodecyl sulfate (SDS) equilibration is done on the same stage without moving the gel. The IEF stage is then moved horizontally to couple with a precast second dimensional gel. The <0.5 mm gap between the two gels is filled with poly (ethylene oxide) solution. After SDS-polyacrylamide gel electrophoresis separation, a charge-coupled device camera is used to detect spots via protein native fluorescence excited by a Hg (Xe) lamp with the gel inside the running cell. Potential for full automation is demonstrated with 0.5 μg of *Escherichia coli* proteins on this miniaturized platform. More than 240 spots are detected in a total experiment time of <2.5 h.

* Adapted with permission from Journal of Chromatography A, 1087(2005) 177-182

Introduction

Proteins are directly responsible for cellular structure and function. Proteomics, focusing on the large-scale identification and quantification of proteins, is an important area for bioanalytical chemistry[1, 2]. To date, most separations of complex protein mixtures are carried out using two-dimensional gel electrophoresis (2D-GE)[3-7]. In O'Farrell's original paper[8], in vivo ^{14}C- or ^{35}S-labeled proteins from *Esherichia coli* were first separated in a glass tube according to their isoelectric points (pI) by isoelectric focusing (IEF) with carrier ampholytes. The IEF gel was extruded after protein focusing and equilibrated with sodium dodecyl sulfate (SDS) buffer. The cylindrical gel was then laid on top of the second dimensional slab gel and kept in place by 1% agarose to separate proteins according to molecular weight. Slab gels were dried after separation and detected by autoradiography. About 1100 protein spots were detected. This high resolution, however, comes at the expense of intensive labor, long operation time and low reproducibility. The experiment requires meticulous handling of the delicate gels, and takes days to finish. Sample handling, gradient drifting over prolonged focusing, and gel deformation during extrusion all contribute to run-to-run variation.

Technological improvements over the last three decades have greatly simplified 2D-GE separation and protein detection. Tube gels were replaced with immobilized pH gradient-gel strips bonded on a plastic film[9]. This greatly facilitated gel handling. Radioactive labeling, plagued by biohazard concerns and days of exposure time[10, 11], is gradually replaced by more environmentally-friendly and fast-staining or fluorescence-labeling methods. With specially designed instruments, separation and detection can be completed in a day on a mini size (6–8 cm) gel.

However, the labor-intensive and time-consuming nature of traditional 2D-GE has not been improved. Protein laboratories are still transferring gels with tweezers in and out of buffers and holders. Gels of smaller size and thickness, which offer even faster separation due to improved heat dissipation[12, 13], are seldom used not only because of the lack of detection systems sensitive enough for the low-abundance proteins, but also because of the lack of automation and thus insufficient precision[12].

Increasingly, liquid-based multidimensional liquid chromatography (LC), capillary electrophoresis (CE), and LC-CE are used in peptide and protein separation[14-17] because of the availability of automated instrumentation. Different combinations of LC modes have been used for proteins separation, such as ion-exchange and reversed-phase (IEC-RPLC)[18, 19], size-exclusion and reversed-phase (SEC-RPLC)[20, 21], and ion-exchange and size-exclusion (IEC-SEC)[22]. A prime demonstration published recently is the multidimensional protein identification technique (MudPIT), developed in the Yates' group[23]. Using a step-gradient, trypsin digested proteins are separated by strong cation exchanger (SCX) and reversed-phase stationary phases that are packed in a single fused-silica capillary in series, and directly analyzed by mass spectrometry (MS) or tandem MS via electrospray ionization. Thousands of proteins can be identified within a few hours by database searching. RPLC are also coupled with electrophoresis for peptide and protein separation[24-27]. Multidimensional CE protein separations based on principles other than the combination of IEF and SDS-GE have also been performed[28-32]. Moreover, although most of the methods have peak capacity comparable with or even higher than traditional 2D-GE, the 2D-in-time configurations generally involve some resolution compromise because of the low sampling frequency of the second dimension comparing to the peak widths of the first dimension[33].

Despite fast separation and automation, the above methods do not provide p*I* or molecular weight information that can be directly related to databases familiar to biologists. The lack of databases for methods other than 2D-GE makes MS the necessary detector for protein identification. Also, although the common digestion-before-separation approach in these methods is potentially helpful for fast protein mapping and/or for biological marker identification when combined with MS, important protein information, exemplified by protein quantity and post-translational modifications (especially multiple modifications on the same tryptic peptide), tends to be missed. 2D polyacrylamide gel electrophoresis (PAGE), however, is known to work well if the goal is to look for protein modification and/or quantitative change (up or down regulation)[34]

To take advantage of both the large database of 2D-GE and the fast, automatable separation of CE, traditional 2D-GE has been converted to the capillary format with polymer solutions as the anti-convection and sieving matrix[35, 36]. Some schemes even use parallel separation in the second dimension to further increase the throughput[37, 38]. However, band broadening due to either heterogeneity caused by labeling or distorted electric field distribution during protein transfer are observed.

The direct pI and molecular weight information, the large database available, and the low operational cost have greatly favored 2D-GE over other protein separation and detection methods. It is the low degree of automation that hindered traditional 2D-GE's application in modern day protein analysis. Full automation will be a major advance in 2D-GE development and the inherent high throughput of a fully automated system will definitely further consolidate its role in proteomics. Here, we demonstrate an integrated 2D-GE system that is ready to for full

automation. Sample application and first dimensional separation, IEF, are performed on a discrete stage without special holders. Coupling this to the second dimensional gels is accomplished by moving the IEF strip linearly and filling the gap with poly(ethylene oxide) (PEO) solution. The whole running cell is directly put under a UV lamp and spots are detected with a charge-coupled device (CCD) camera via protein native fluorescence[39-41].

Experimental section

Chemicals and samples

Sample proteins from *E. coli*, carrier ampholytes (Bio-Lyte 3/10, Bio-Lyte 5/7), urea, dithiothreitol (DTT), 3-[3-(cholamidopropyl)dimethylammonio]-1-propanesulfonate (CHAPS), acrylamide and bisacrylamide mixture (3.3% crosslinker), 1.5 M Tris–HCl solution (pH 8.8), 0.5 M Tris–HCl solution (pH 6.8), and SDS-PAGE running buffer were obtained from Bio-Rad (Hercules, CA, USA). Dry IEF gels and agarose were purchased from Amersham Biosciences (Piscataway, NJ, USA). SDS, ammonium persulfate, *N*,*N*,*N*′,*N*′-tetramethylethylenediamine (TEMED), PEO (M_r 8,000,000), and glycerol were purchased from Sigma (St. Louis, MO, USA). SDS running buffer is obtained from Bio-Rad and diluted according to the manufacturer's instructions. All electrodes were made of platinum wire (0.25 mm diameter) from Surepure Chemetals (Florham Park, NJ, USA).

2D GE cell design

The designed platform for 2D-GE adopts a horizontal format, as shown in Figure 1. Part I (Figure 1A) includes the 3-mm wide IEF stage and the cathodic buffer well for the second (SDS-PAGE) dimension. The embedded IEF electrodes, 10 mm apart, are wired from the bottom and protrude only 0.1 mm on the stage. IEF strip, 1 mm × 19 mm with only 11 mm dry gel in the center, is placed facing down along the edge of the stage before the experiment. Both bare plastic ends of the strip are clamped on the 0.4 mm high steps at the two sides of the IEF stage. Part II (Figure 1B) includes the 20 mm × 20 mm slab gel cassette stage, extension pocket, and the anodic buffer well for SDS-PAGE. The gel cassette is made of low UV fluorescence bottom glass, 20 mm × 4 mm × 0.75 mm thick spacers, and fused-silica cover glass. Gels are cast before experiments. The slab gel consists of a 3-mm stacking gel (4%) and a 12-mm resolving gel (12%) buffered at the same pH and ionic strength (pH 8.8 and 0.375 M Tris–HCl). The cassette glass choice is necessary for direct native fluorescence excitation and detection. A 14 mm × 14 mm opening is cut through the center of the stage to reduce the background fluorescence. The gel cassette is held tightly against the stage by clamps on the sides. Glue or rubber gasket can be used between the stage and gel cassette to prevent leaking. The extension pocket fits the IEF stage of Part I. The two parts are aligned 2 mm apart, creating a temporary void before experiments (Figure 1A). Both parts are made of Delrin®.

Detection system

Details of the native fluorescence detection setup are described elsewhere[13]. Native fluorescence detection eliminates the staining and destaining steps. It can be implemented by direct excitation through quartz plates. Briefly, collimated light from a Hg (Xe) lamp is selected

by a set of filters to give 270–320 nm excitation band at about 1 mW/cm^2. The fluorescence signal passing through emission filter set (>320 nm), is collected by a UV camera lens and detected by a cooled CCD camera. We have shown previously that this system is capable of detecting a protein spot of 0.04 ng.

Experimental protocol

The integrated operation can be divided into three steps.

Sample application and IEF

Five microliters of rehydration solution (containing 0.1 μg/μL sample protein, 8 M urea, 1.5% CHAPS, 1.8% Bio-Lyte 5/7, 1.2% Bio-Lyte 3/10, 0.3% freshly added DTT) is pipetted along the inner edge of the dry gel strip onto the IEF stage. The solution is readily drawn under the strip by capillary action. Then, the cassette is placed on top of a thermoelectric cooler (Advanced Thermoelectric, Nashua, NH, USA). The temperature is set at 18 °C. The electrophoretic cell is put under a polycarbonate cover with an open container filled with water alongside. Both temperature and humidity are maintained for the 1 h gel rehydration and the subsequent IEF. IEF is performed directly after rehydration at 75 V for 4 min, 200 V for 4 min, 300 V for 10 min, and 400 V for 30 min. Total IEF is no more than 280 V h. Current decreases steadily for the period of constant voltage except for the last 5–10 min, where current stays at around 20 μA.

Coupling of the two-dimensional gels

Sixty microliters equilibration solution (containing 2% SDS, 60 mM Tris–HCl at pH 6.8, 10% (v/v) glycerol, 1% freshly prepared DTT) is added on the IEF stage along the gel strip. The SDS and protein are allowed to interact for 15 min. Then, 0.2 mL of 2% (w/v) PEO solution [containing 0.05% (w/v) bromophenol blue] is added into the temporary well from the side channel with a syringe. Tightening the alignment screws couples the two blocks together and gradually reduces the volume of the well, squeezing the PEO solution up to connect the two gels (Figure 1B). A rubber gasket is added between the two parts to prevent possible leaking during SDS-PAGE. A photograph of the entire assembly is shown in Figure 2.

SDS-PAGE and protein detection

About 2 mL of 1× Tris/glycine/SDS is added to each buffer well to merge over the IEF strip but not over the cover glass. Twenty millimeters long electrode pairs are dipped into the buffer wells parallel to the IEF gel. SDS-PAGE is carried out at 100 V for about 7 min utill the bromophenol blue marker line migrates out of the gel. Buffer solution is drained and the cover glass is flushed with DI water and air-dried before the whole unit is put under the detection setup for imaging. The exposure time is set to 2 min.

Results and discussion

Performance of the device

An image of the second dimensional gel is shown in Figure 3. Two hundred and forty-four spots are detected with the 2D image analysis software PDquest from Bio-Rad. This

represents better detection sensitivity for native fluorescence detection than previously reported[13]. The reason might be that protein loss due to gel rinsing after separation is eliminated since the gel is directly detected inside the glass cassette. However, the spot number is still a bit lower than conventional mini gel (7 cm IEF and 6 cm SDS-PAGE), where ~300 spots are detected[13]. This is mainly because the loading amount is 40 times lower in the small gel than the conventional one. Low loading can be useful since the biological samples are usually quite limited.

Automation potential of the device

The experimental design outlined is based on the potential for full automation. The flexible nature of polyacrylamide gels poses the biggest challenge for automating the separation. Running both dimensions on a single gel would be the best approach. However, unless there is an effective way to confine the proteins from spreading perpendicularly to the IEF electrical field, a 2D-on-one-gel configuration is not feasible. To ensure proper focusing of protein, the two gels have to be separated during the IEF step. We first tried to set the IEF gel at a small distance (~1 mm) from the slab gel during IEF and sealed the gap afterwards with agarose solution (before SDS-PAGE). It works well if the sample loading step is performed off-line. Rehydration and loading in situ often causes current leakage due to sample solution diffusion. Protein focusing is thus not reproducible. Even if there is no current leakage and the proteins are focused well, the slab gel fluorescence image tends to have higher background, presumably because the portion of the sample proteins that are not absorbed by the IEF gel and are thus not focused also migrated into the second dimensional gel. Severe horizontal streaking is observed in the case of cup loading, where the dry IEF gel is rehydrated off-line. This also means handling of the

hydrated gels. We thus decide to physically isolate the gel strip from the slab gel during isoelectric focusing and couple the two gels by moving the two parts of the rigid running cell instead of the two flexible gels.

To automate the step of sample loading and first dimensional electrophoresis, the strip gel is designed to be loaded onto the IEF stage before sample application. Mounting the strip with the gel side facing down exploits capillary action to drive the sample solution underneath the gel for proper gel rehydration and protein loading. Rehydration and loading now becomes analogous to sample injection and can be performed by a computer-controlled syringe through a channel in the cassette.

Integrating the IEF electrodes into the IEF stage helps to avoid the hassle of positioning them before IEF and in the removal afterwards. However, the traditional parallel IEF electrodes generate a considerable amount of bubbles during the second dimensional electrophoresis, thereby interrupting the separation. Here, a pair of tiny pin electrodes are used. These do not generate noticeable bubbles under the experimental conditions used due to the reduced surface area. To facilitate the coupling of the two gels, IEF is performed on one edge of an open, flat surface instead of inside a traditional holder, where rehydration solution and individual IEF strip gel are isolated and cover by a layer of mineral oil. Humidity control, however, becomes crucial to ensure proper gel rehydration and protein focusing since a very small volume of rehydration solution is applied. We found that air saturated with water vapor is as good as cover oil for preventing evaporation.

Direct coupling the two-dimensional gels can be very simple if no SDS equilibration is required. Although IEF gels can be coupled directly with the second dimension slab gel without

a SDS equilibration step, it usually causes severe vertical streaking due to incomplete SDS–protein binding[42]. With the gel strip poised on the edge of IEF stage, SDS buffer can be directly added onto the stage. Handling the gel strip in and out of solution is avoided. The SDS buffer does not need to be removed because the composition is similar to the second dimensional running buffer. After SDS equilibration, the IEF stage is brought to close contact with the slab gel stage. However, due to the casting process employed, there is still a ~0.5 mm gap between the two gels. 2% PEO solution is used instead of the traditional agarose gel to avoid the prior melting step. Because of its high viscosity, the PEO solution cannot only be held in the make-shift well temporarily without leaking out, but also connects the two gels without being diluted by the equilibration solution or the running buffer before protein transfer is completed. Thus, with two computer-controlled syringes to dispense SDS equilibration buffer and PEO solution, and one motorized stage attached to either part of the cassette, the 2D coupling step can be automated.

The second dimensional electrodes can be also integrated into the buffer wells since they do not interfere with the first dimensional separation. The liquid level in both of the wells can be regulated by a pair of pressure valves. Water flushing and air drying of the cover-glass surface can also be done in situ before detection. Direct spot detection by protein native fluorescence with the gel inside the electrophoresis cell represents the simplest detection mode. Due to ubiquitous UV fluorescence of the cassette, it is essential to create an opening at the center of the slab gel cassette stage to reduce the background noise for detecting the low signal from proteins. This also benefits heat dissipation during the second dimensional electrophoresis because the cooling unit can be in direct contact with the bottom glass. Moreover, the distinct noise spots in

the gel images[13] are greatly reduced because dust particles, the presumed major source responsible for the spots, attach more easily to the exposed gel than to the glass surface.

Conclusions

The simple design demonstrated above is capable of automated 2D-GE separation and detection without complicated robotic operations. The most expensive instrumental component required would be a CCD camera, but that is not much more costly than a high resolution scanner typically used for gel scanning. In a commercial version of this system, one would have the two disposable blocks of the cassette manufactured with the two gels precast onto them. We note that prepared IEF strips and precast SDS-PAGE gels are already commercially available in sealed packages in larger formats.

Traditional 2D-GE has been used both for differential expression profiling in analytical scale and isolating pure proteins in preparative scale. Miniaturized automatic 2D-GE can thus be used in differential expression experiments, such as disease diagnosis or drug response assay, as a complementary technique to protein microarrays. Horizontal expansion of the current design will allow processing several gels in parallel. For example, the hydration steps can be done in parallel off-line to achieve high throughput preparation. Robotics can then be employed to mate the focused (IEF) gel blocks to the SDS-PAGE gel block sequentially for size separation and detection at the optical module. Although the suitability for automation of this design is demonstrated in a miniaturized format, it can easily be scaled up for higher loading capacity

when low abundance proteins are of interest and the detection sensitivity is limited, or if proteins are to be isolated.

Despite these advantages, an automated system solves only part of the problems facing 2D-GE. Improvement of cell proteome coverage, especially proteins with high molecular weight, high hydrophobicity, and extreme pI values, will need further development. Detection of low abundance proteins, particularly with limited sample amounts, is another critical issue for both 2D-GE and other proteomics methods. It is also important to combine automated separation and detection with new techniques that link gel proteins with MS when protein identification is desired. When new protein spots are detected, MS or MS/MS is usually performed to identify these spots. The current gel-protein MS identification method involves multiple operation steps, typically including spot excision, proteolytic digestion, peptide extraction/concentration, and repeated washing and drying. Simple but efficient protein transfer from gel to MS, such as the integration of electronic protein transfer and membrane proteolytic digestion[43], are challenges that require additional development of the integrated system reported here.

Acknowledgement

E.S.Y. thanks the Robert Allen Wright Endowment for Excellence for support. The Ames Laboratory is operated for the US Department of Energy by Iowa State University under Contract No. W-7405-Eng-82. This work was supported by the Director of Science, Office of Basic Energy Sciences, Division of Chemical Sciences.

References

(1) Velculescu, V. E.; Zhang, L.; Vogelstein, B.; Kinzler, K. W. *Science (Washington, DC, U. S.)* **1995**, *270*, 484-487.

(2) Pandey, A.; Mann, M. *Nature (London, U. K.)* **2000**, *405*, 837-846.

(3) Kuster, B.; Krogh, T. N.; Mortz, E.; Harvey, D. J. *Proteomics* **2001**, *1*, 350-361.

(4) Molloy, M. P. *Anal. Biochem.* **2000**, *280*, 1-10.

(5) Sanchez, J. C.; Chiappe, D.; Converset, V.; Hoogland, C.; Binz, P. A.; Paesano, S.; Appel, R. D.; Wang, S.; Sennitt, M.; Nolan, A.; Cawthorne, M. A.; Hochstrasser, D. F. *Proteomics* **2001**, *1*, 136-163.

(6) Nilsson, C. L.; Larsson, T.; Gustafsson, E.; Karlsson, K. A.; Davidsson, P. *Anal. Chem.* **2000**, *72*, 2148-2153.

(7) Bichsel, V. E.; Liotta, L. A.; Petricoin, E. F. *Cancer J.* **2001**, *7*, 69-78.

(8) O'Farrell, P. H. *J. Biol. Chem.* **1975**, *250*, 4007-4021.

(9) Bjellqvist, B.; Ek, K.; Giorgio Righetti, P.; Gianazza, E.; Gorg, A.; Westermeier, R.; Postel, W. *J. Biochem. Biophys. Methods* **1982**, *6*, 317-339.

(10) Steinberg, J. *J. NIH Res.* **1996**, *8*, 30-36.

(11) Yeargin, J.; Haas, M. *Curr. Biol.* **1995**, *5*, 423-431.

(12) Neuhoff, V. *Electrophoresis* **2000**, *21*, 3-11.

(13) Sluszny, C.; Yeung, E. S. *Anal. Chem.* **2004**, *76*, 1359-1365.

(14) Larmann, J. P.; Lemmo, A. V.; Moore, A. W.; Jorgenson, J. W. *Electrophoresis* **1993**, *14*, 439-447.

(15) Evans, C. R.; Jorgenson, J. W. *Anal. Bioanal. Chem.* **2004**, *378*, 1952-1961.

(16) Quigley, W. W. C.; Dovichi, N. J. *Anal. Chem.* **2004**, *76*, 4645-4658.

(17) Hu, S.; Michels, D. A.; Fazal, M. A.; Ratisoontorn, C.; Cunningham, M. L.; Dovichi, N. J. *Anal. Chem.* **2004**, *76*, 4044-4049.

(18) Opiteck, G. J.; Lewis, K. C.; Jorgenson, J. W.; Anderegg, R. J. *Anal. Chem.* **1997**, *69*, 1518-1524.

(19) Wagner, K.; Miliotis, T.; Marko-Varga, G.; Bischoff, R.; Unger, K. K. *Anal. Chem.* **2002**, *74*, 809-820.

(20) Opiteck, G. J.; Jorgenson, J. W.; Anderegg, R. J. *Anal. Chem.* **1997**, *69*, 2283-2291.

(21) Stroink, T.; Wiese, G.; Lingeman, H.; Bult, A.; Underberg, W. J. M. *Anal. Chim. Acta* **2001**, *444*, 193-203.

(22) Bushey, M. M.; Jorgenson, J. W. *Anal. Chem.* **1990**, *62*, 161-167.

(23) Wolters, D. A.; Washburn, M. P.; Yates, J. R. *Anal. Chem.* **2001**, *73*, 5683-5690.

(24) Tragas, C.; Pawliszyn, J. *Electrophoresis* **2000**, *21*, 227-237.

(25) Zhou, F.; Johnston, M. V. *Anal. Chem.* **2004**, *76*, 2734-2740.

(26) Chen, J. Z.; Balgley, B. M.; DeVoe, D. L.; Lee, C. S. *Anal. Chem.* **2003**, *75*, 3145-3152.

(27) Moritz, R. L.; Ji, H.; Schutz, F.; Connolly, L. M.; Kapp, E. A.; Speed, T. P.; Simpson, R. J. *Anal. Chem.* **2004**, *76*, 4811-4824.

(28) Yang, C.; Zhang, L.; Liu, H.; Zhang, W.; Zhang, Y. *J. Chromatogr., A* **2003**, *1018*, 97-103.

(29) Mohan, D.; Lee, C. S. *Electrophoresis* **2002**, *23*, 3160-3167.

(30) Sheng, L.; Pawliszyn, J. *Analyst* **2002**, *127*, 1159-1163.

(31) Michels, D. A.; Hu, S.; Schoenherr, R. M.; Eggertson, M. J.; Dovichi, N. J. *Mol. Cell. Proteomics* **2002**, *1*, 69-74.

(32) Herr, A. E.; Molho, J. I.; Drouvalakis, K. A.; Mikkelsen, J. C.; Utz, P. J.; Santiago, J. G.; Kenny, T. W. *Anal. Chem.* **2003**, *75*, 1180-1187.

(33) Murphy, R. E.; Schure, M. R.; Foley, J. P. *Anal. Chem.* **1998**, *70*, 1585-1594.

(34) Rabilloud, T. *Proteomics* **2002**, *2*, 3-10.

(35) Yang, C.; Liu, H.; Yang, Q.; Zhang, L.; Zhang, W.; Zhang, Y. *Anal. Chem.* **2003**, *75*, 215-218.

(36) Wang, Y. C.; Choi, M. H.; Han, J. *Anal. Chem.* **2004**, *76*, 4426-4431.

(37) Chen, X.; Wu, H.; Mao, C.; Whitesides, G. M. *Anal. Chem.* **2002**, *74*, 1772-1778.

(38) Li, Y.; Buch, J. S.; Rosenberger, F.; DeVoe, D. L.; Lee, C. S. *Anal. Chem.* **2004**, *76*, 742-748.

(39) Lee, T. T.; Yeung, E. S. *Anal. Chem.* **1992**, *64*, 3045-3051.

(40) Lee, T. T.; Lillard, S. J.; Yeung, E. S. *Electrophoresis* **1993**, *14*, 429-438.

(41) Chang, H. T.; Yeung, E. S. *Anal. Chem.* **1993**, *65*, 2947-2951.

(42) Gorg, A.; Postel, W.; Gunther, S.; Friedrich, C. *Electrophoresis* **1988**, *9*, 57-59.

(43) Cooper, J. W.; Lee, C. S. *Anal. Chem.* **2004**, *76*, 2196-2202.

Figure captions

Figure 1. Schematic diagram of integrated 2D-GE cassette. (A) Assembly of Part I (left block) for IEF with dry strip in green and Part II (right block) for SDS-PAGE with gel in blue: two parts are separated with 2-mm gap; buffer wells on both sides are empty for first dimensional separation; and (B) assembly fitted together and buffer wells filled with SDS buffer for second dimensional separation.

Figure 2. 2D-GE platform. The overall dimension is 5 cm × 7 cm. Two millimeters spacers are used to isolate the two parts during first dimensional separation and are removed before mating the two parts together for the second dimensional separation.

Figure 3. Native fluorescence gel image of 0.5 μg *E. coli* proteins. The entire gel is 11 mm × 11 mm.

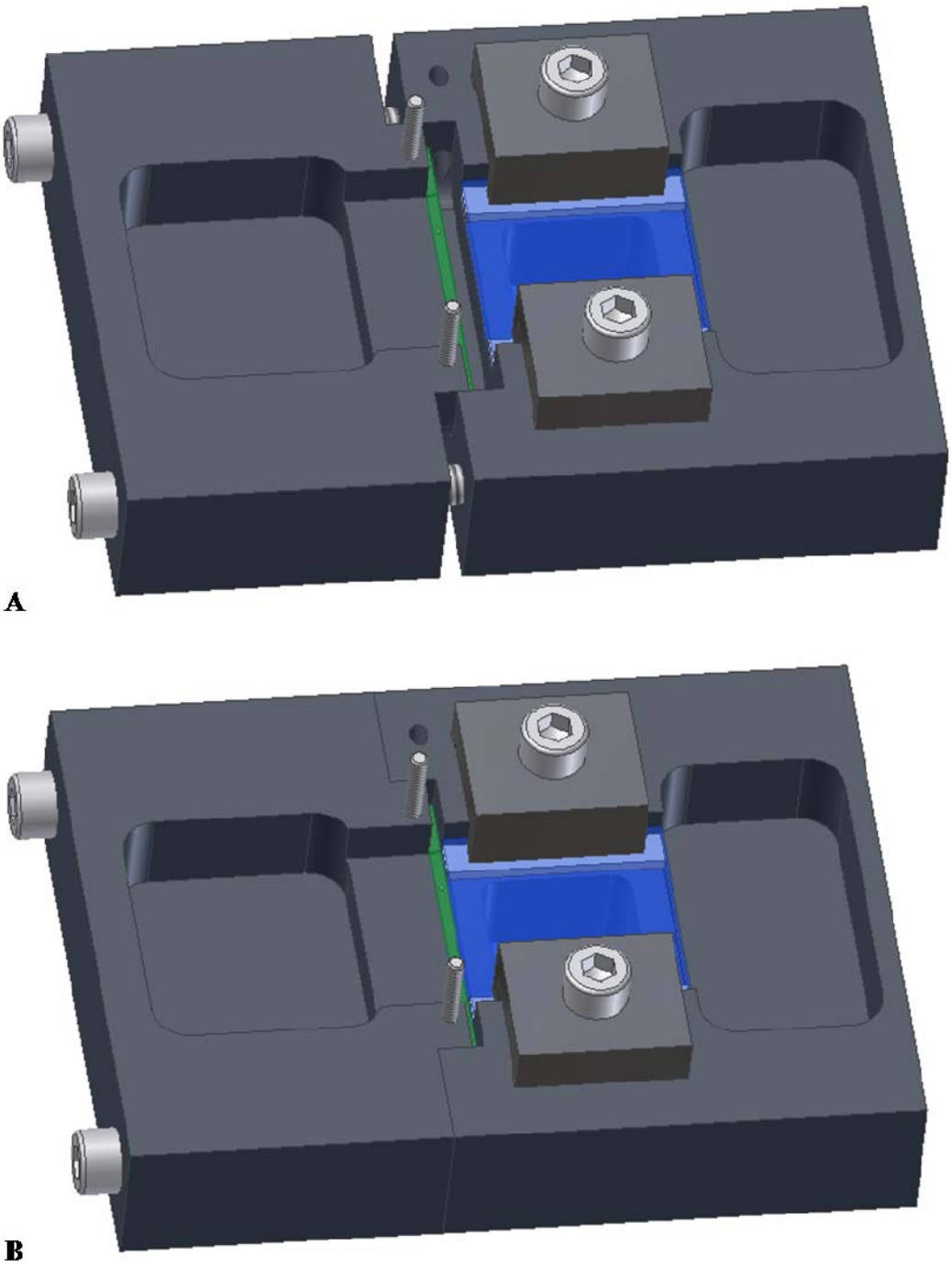

Figure 1

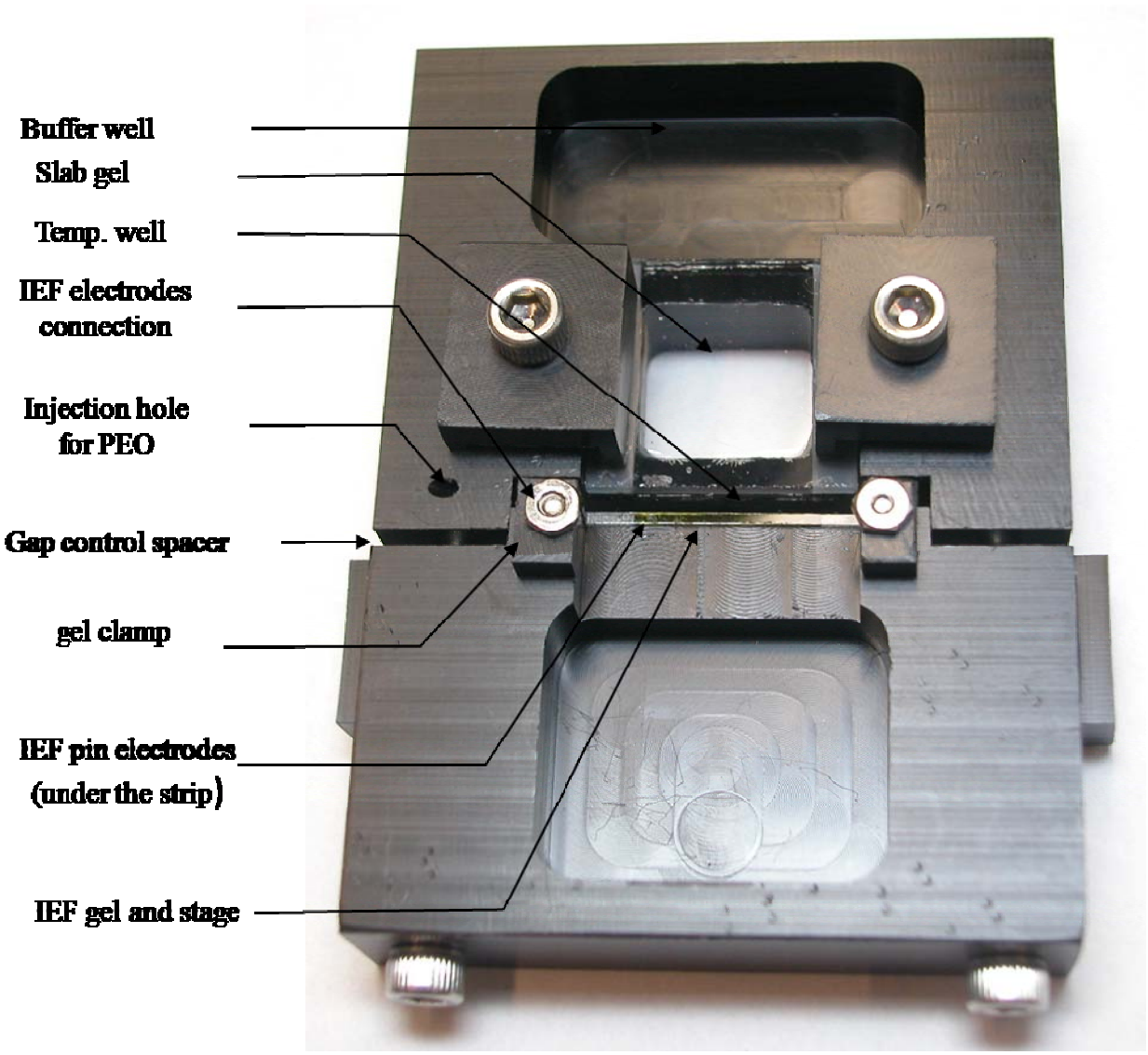
Buffer well
Slab gel
Temp. well
IEF electrodes connection
Injection hole for PEO
Gap control spacer
gel clamp
IEF pin electrodes (under the strip)
IEF gel and stage

Figure 2

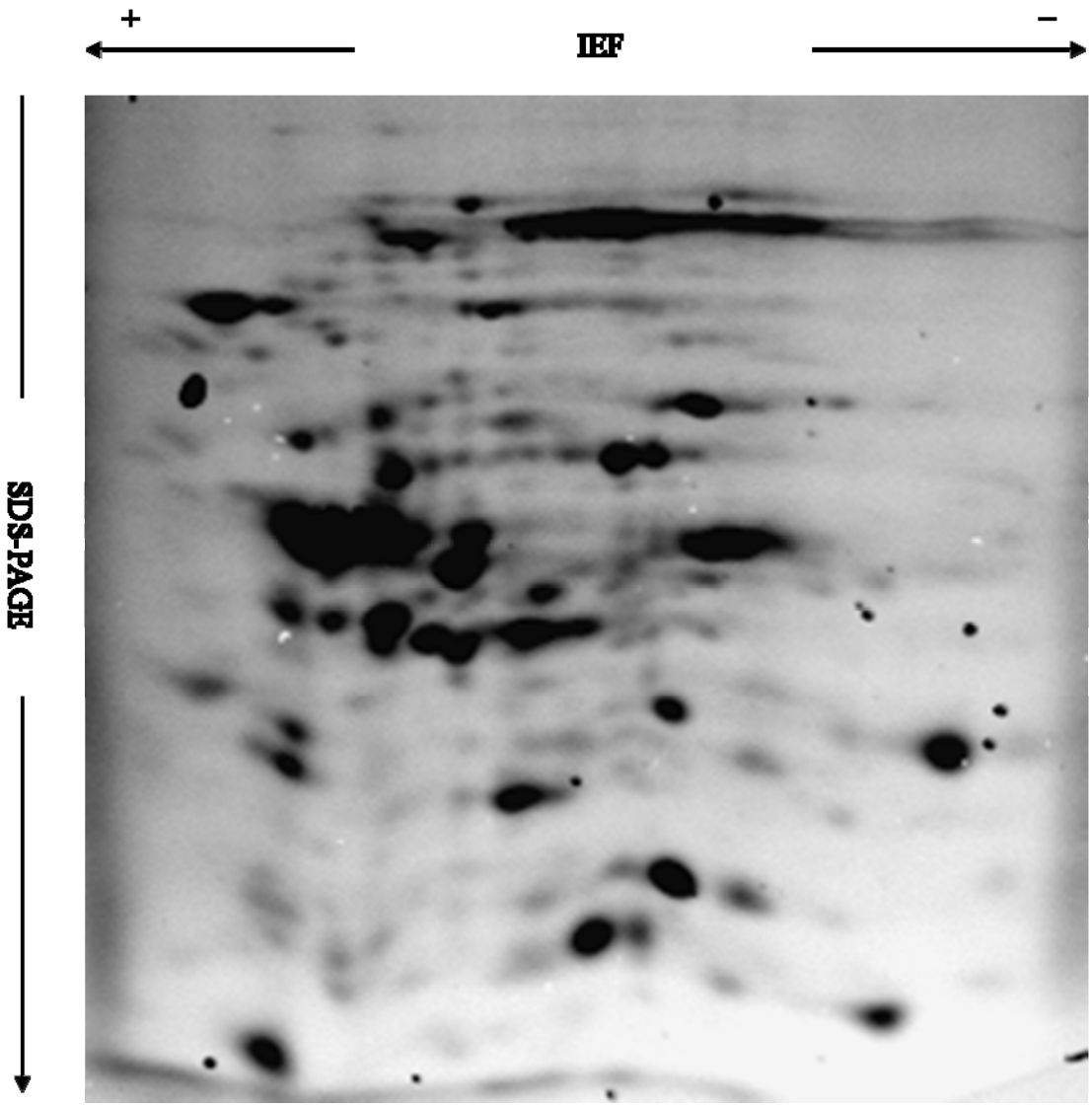

Figure 3

CHAPTER 3. DETERMINATION OF NAD^+ AND NADH LEVEL IN A SINGLE CELL UNDER H_2O_2 STRESS BY CAPILLARY ELECTROPHORESIS

A paper prepared for submission to Analytical Chemistry

Xenjun Xie, Aoshuang Xu, and Edward S. Yeung

ABSTRACT

A capillary electrophoresis (CE) method is developed to determine the levels of both β-nicotinamide adenine dinucleotide (NAD^+) and its reduced form, NADH, in single cells based on an enzymatic cycling reaction. Detection limit as low as 0.2 amol of NAD^+ and 1 amol of NADH was achieved with a home-made laser induced fluorescence (LIF) setup. The method showed good reproducibility and specificity. After an intact cell was injected into the inlet of a capillary and lysed using a Tesla coil, intracellular NAD^+ and NADH were separated, incubated with the cycling buffer, and quantified by the amount of fluorescent product generated. The levels of NAD^+ and NADH of cells from three cell lines and one primary astrocytes culture were determined using this method. By comparing NAD^+ and NADH levels of cells exposed to oxidative stress imposed by H_2O_2 to those without exposure, we find that H9c2 cells respond to the stimuli by activating the DNA repair enzyme poly(ADP-ribose) polymerases, while astrocytes respond by increasing cellular NADH/NAD^+ ratio.

INTRODUCTION

β-nicotinamide adenine dinucleotide, NAD^+, and its reduced form, NADH, are ubiquitous and important biomolecules found in both eukaryotic and prokaryotic organisms. As coenzymes of numerous oxidoreductases[1], they transfer hydrogen atoms and electrons from one metabolite to another in many cellular redox reactions. Particularly, NAD^+ and NADH are involved in cellular energy metabolism including glycolysis, TCA cycle, and oxidative phosphorylation, hence they are essential to the synthesis of ATP. NAD^+ and NADH also play an important role in calcium homeostasis, DNA repair, and gene expression[2] by functioning as a substrate for three other classes of enzymes: 1) ADP-ribose transferases (ARTs) or poly(ADP-ribose) polymerases (PARPs), 2) cADP-ribose synthases, and 3) sirtuins (histone deacetylases)[3].

The NADH/NAD^+ ratio is an indicator of cellular metabolic status. It regulates the cell redox state via enzymes such as the glycolytic enzymes and the pyruvate dehydrogenase involved in acetyl-CoA synthesis in TCA cycle[4]. It has been reported[2, 5, 6] that under oxidative stress imposed by H_2O_2 some cell types (erythrocyte, for example) increase their intracellular NADH/NAD^+ ratio or their NADH level in order to resist possible oxidative damage. Meanwhile, cell apoptotic mechanism studies[7-10] have suggested that the exposure of cells to H_2O_2 leads to DNA single strand breakage and subsequently the activation of the DNA repair enzyme – PARPs. PARPs consume NAD^+ to form branched polymers of ADP-ribose on target proteins involved in DNA repair. The extensive activation of PARPs may cause a critical reduction of cellular NAD^+ level and ultimately cell death.

Intracellular NAD^+ and NADH levels are also related to cell proliferation[11], sickle cell disease[12], tumor development[13], neoplasia and ischaemia[14], and a number of brain diseases[3]. Investigation of cellular NAD^+ and NADH levels and their variation in response to different environmental stimuli has been an important subject in biology, biochemistry and medicine. Pogue et al.[15], for instance, have used NADH as a marker to assess cellular damage in tissues caused by photodynamic therapy (PDT), and found that the decrease in NADH was correlated to the PDT dose applied.

The total concentration of NAD^+ and NADH in most cells is in the range of 10^{-3} M to 10^{-6} M with a ratio of NAD^+/NADH varying from 1 to 700[4]. These nucleotides are found in cytosol, mitochondria, peroxisomes, and other cellular compartments. They can either exist in free form or bound to enzymes. Several methods are currently available for the determination of NAD^+ and NADH in organelles, cells, and tissues.

Traditionally, quantification of cellular NAD^+ and NADH has been performed on the extract of a population of cells with HPLC separation coupled with UV absorption[16-18], fluorescence[18], or mass spectrometry[19] detection, or with enzymatic assay coupled with colorimetry[20-22] or fluorometry[23-26]. Since quantification with HPLC-UV is rather insensitive, having only mM level concentration detection limit of NAD^+ yet requiring μL level of cell extract, a large number of cells are required. Fluorescence of NADH or mass spectrometry is more sensitive, but still gives only pmol level mass detection limit. Standard enzymatic assay takes advantage of the fluorescence of NADH centered at 460nm, measuring NADH by monitoring the decrease of fluorescence signal while NADH is enzymatically oxidized to NAD^+ and measuring NAD^+ by monitoring the

signal increase while NAD^+ is oxidized to NADH. The minimum requirement of μL level of sample also makes standard enzymatic assay a rather low sensitivity approach.

By coupling two enzymatic reactions, one reduces NAD^+ to NADH and the other oxidizes NADH to NAD^+, a sensitive enzymatic cycling assay of NAD^+ and NADH was developed as early as 1961[20]. Early enzymatic cycling assays[20-22] use absorptive dyes as end-products and can detect NAD^+ or NADH down to the pmol level; more recently, fluorescent end-products[23-26] were employed to give even better sensitivity (0.2 nM of NAD^+ in a 200 μL reaction volume[23]). Since these enzymatic cycling assays do not distinguish NAD^+ from NADH, two extractions however are needed in order to quantify them separately. NAD^+ is usually extracted in an acidic solution to eliminate NADH; NADH is extracted in an alkaline solution, which eliminate NAD^+.

Overall, these extraction based approaches do not demand extreme detection sensitivity and can work well when the measured population can be assumed to be relative homogeneous. However, biochemical processes of cells, even those from the same tissue or organ, are not always synchronized, and homogeneity of cells cannot always be assumed[27]. Additionally, many diseases such as cancer start from only a few cells; with bulk analysis the signal from these abnormal cells are very likely to be masked by the large number of surrounding normal cells, making it difficult to diagnose the diseases at an early stage[28]. Knowledge of biochemistry at single cell level is crucial to understand complex processes such as cell communication and biological response to external stimuli.

Imaging fluorescence microscopy has been used to measure NADH in cells without extraction. Both one-photon UVA excitation and two-photon NIR excitation[29-31]

have been used. The approach has much better sensitivity to observe even sub-cellular distribution of NADH and can be used for *in vivo* studies. For example, Karl et al.[32] utilized two-photon NADH fluorescence microscopy to study the live metabolic process in neurons and astrocytes during focal neural activity. However, the strong scattering and background fluorescence can make quantification unreliable. Ramanujan et al.[33] recently used multi-photon fluorescence lifetime imaging in the time domain to discriminate against the background auto-fluorescence. However the non-fluorescent NAD^+ cannot be measured by this approach.

The combination of small sampling volume (nL to pL), high resolution separation, and the availability of sensitive detection (such as laser induced fluorescence) has made CE one attractive tool in the analysis of components from single cells. CE single cell analysis is usually carried out by lysing individual cells in a small inner diameter (I. D.) capillary, followed by separation of the lysate and detection of the species of interest. Since the analytes can be separated from other intracellular species directly after a cell is lysed in the capillary, extra manipulation and dilution, often necessary with bulk extraction approach, are minimized and very low amounts of cellular and even sub-cellular components can be detected. CE has been used to determine different classes of intracellular components in single cells, such as amino acid[27], peptide[34],proteins[35-37], and neurotransmitters[38].

Additionally, the small volume of a capillary is advantageous when CE is coupled to a chemical reaction. The reaction can be done inside the capillary with minimal dilution; the reagents and products are monitored directly by electrophoretic separation and transportation to the detector. This “nano-reactor” feature of the capillary has been

exploited in a host of applications of CE such as DNA sequencing[39], peptide mass fingerprinting[40], immunoassay[41], and enzyme assay[42]. In fact, on-line derivatization of species of interest with highly fluorescent labels has been one of the most successful strategies in single cell analysis[43]. Coupling of CE-LIF with enzymatic cycling would likely provide sufficient sensitivity for single cell NAD^+ and NADH analysis.

In this study, a method of in-capillary enzymatic cycling assay is developed to determine NAD^+ and NADH content of a single cell. The method is applied to study cell NAD^+ and NADH level change in response to oxidative stress caused by hydrogen peroxide.

Experimental section

Reagents and chemicals

Lactate dehydrogenase (LDH, EC 1.1.1.27) was purchased from Calzyme Laboratories Inc (San Luis Obispo, CA, USA). Diaphorase (DIA, EC 1.6.99.-) was purchased from Shinko American Inc (New York, NY, USA). LDH and DIA were dialyzed against 20 mM sodium phosphate buffer for 24 hours before use. Resazurin was purchased from Invitrogen (Carlsbad, CA, USA) and dissolved in 50 mM pH 7.20 sodium phosphate buffer to make a 1 mM stock solution; this stock solution is extracted with chloroform at 4:6 (v/v) before use. Tris buffer (1.0 M pH 8.5) was purchased from Hampton Research (Aliso Viejo, CA, USA) and diluted to 100 mM without further adjustment. All other chemicals were purchased from Sigma-Aldrich (St. Louis, MO, USA) and used as received. Ultrapure water from a Mili-Q system (Milipore, Billerica, MA, USA) was used throughout experiments.

Cell culture and cell treatment

H9c2, a rat heart myoblast cell line, was purchased from American Type Culture Collection (Rockville, MD, USA) and cultured in Dulbecco's modified Eagle's (DMEM) medium supplemented with 10% fetal bovine serum. Cells were used between Passage 5 and Passage 12 starting from the purchased batch.

Astrocyte primary culture (from rat brain hippocampus) was obtained from Professor Srdija Jeftinija of the Department of Biomedical Sciences at Iowa State University and cultured in DMEM supplemented with 10% fetal bovine serum. Cells were used no later than Passage 5.

For H_2O_2 treatment, cells in a flask were placed in fresh medium and incubated with 100 μM H_2O_2 for 1 hour before harvesting after trypsin treatment. In PARPs inhibition study, 1 mM 3-aminobenzamide was added into the fresh medium 20 min before the addition of H_2O_2. Cell number and viability were assessed via flow cytometry (EasyCD4 System, Guava Technologies, Hayward, CA, USA).

NAD^+ and NADH extraction

The harvested cells were rinsed with Hank's balanced salt solution (HBSS) twice and centrifuged down at 4.5×1000 rpm for 5 min. The cell pellet was resuspended in either 20% (v/v) trichloric acetic acid aqueous solution (to extract NAD^+) or 1 M potassium hydroxide solution (to extract NADH), placed on ice and processed by a probe sonicator for 1 min. The mixture was heated at 60 °C for 45 min and then centrifuged at 13×1000 rpm for 5 min. The supernatant was diluted in Tris buffer before analysis.

NAD^+ and NADH detection by capillary electrophoresis

NAD^+ and NADH were quantified separately in a single run using the enzymatic cycling assay coupled with capillary electrophoresis. As NAD^+ and NADH carry different charges, the two nucleotides can be separated through capillary electrophoresis and mediate the enzymatic cycling reaction at different positions in the capillary.

Reagents for the cycling reaction, including lactate, resazurin, LDH, and DIA were all include in the CE running buffer (100mM TrisHCl). Standard NAD+ and NADH were dissolved in buffers without enzymes. The capillary was first flushed and filled with the full buffer. Electrophoresis was carried out for 3 min to move NAD^+ and NADH to different location of the capillary after injection of sample (single cell or NAD^+/NADH standards). The electrophoresis was then stopped for 3 or 5 minutes before voltage was turned back on until all the products were driven out. The baseline was allowed to return to the original level at the end of each run.

Capillary electrophoresis instruments

A P/ACE™ capillary electrophoresis system (Beckman Coulter, Fullerton, CA, USA) equipped with a photodiode array (PDA) detector was used for exploratory experiments. A 60 cm long (50cm to detection window) fused silica capillary (Polymicro, Phoenix, AZ, USA) of 30 μm I.D. and 365 μm O.D. was used on this instrument throughout the experiments.

For single cell analysis, a home-made CE-LIF system was set up as illustrated in Figure 1. Briefly, a 2.0 mW He-Na laser (543.5 nm) (Melles Griot, Irvine, CA) was focused with a 1-cm focal length fused silica lens into an 11μm I.D. 150μm O.D. fused silica capillary. Fluorescence was collected at 90° by a 40× objective (Edmund Scientific, Barrington, NJ, USA), through a 568 nm cutoff long-pass filter and a 580±20nm

bandpass filter (Semrock, Rochester, NY, USA), and focused on a side-on photomultiplier tube (PMT) (Model R928, Hamamatsu, Bridgewater, NJ). The analog fluorescence signals collected by the PMT were digitized by a pDaq55 A/D converter (Iotech, Cleveland, OH) and recorded at 2Hz with a home-built Labview program on a PC. A 20 μm I.D. and 365 μm O.D. fused silica capillary with a total length of 72 cm and 54 cm to detection window was used. Polyimide coating of the ground end (anode) of the capillary was removed and the tip was etched with 40% hydrofluoric acid to about 60 μm O.D. This end of the capillary is used for injection and mounted on a 3-D micro-manipulator for easy switching between samples and running buffer. The cathode of the capillary was inserted through a flexible septum into an airtight 20 mL glass buffer vial together with the high voltage electrode. A voltage of -22 kV was used for all electrophoresis on this setup.

Cell injection

Before injection, cells suspended in HBSS buffer were added into a chamber made by attaching an O-ring on a clean glass slide. The chamber was mounted on the stage of a microscope (See Figure 2). Under 60× magnification, the etched capillary tip was moved close to a cell with the 3-D micro-manipulator and the cell was injected into the capillary with a pulse of vacuum, which was created by pulling a 3 mL syringe with needle inserted into the sealed buffer vial at the cathode end of the capillary. The injected cell was allowed to settle down to the capillary wall for about 60 sec after injection. A Tesla coil (Figure 3)was then used to lyse the cell for 5 seconds. The capillary was then lifted up from the cell suspension and placed into a glass vial containing the running buffer. The entire process of cell injection takes about 2 minutes.

Standard sample injection

Day-to-day variation was calibrated by injecting standard of NAD^+ and NADH (either alone or mixture), which was prepared in 100 mM Tris buffer (pH 8.5) and injected electrokinetically with -22 kV for 3s.

Statistics

All results except those of single-cell analysis are represented as means ± standard error (SEM) on 3 observations. Student T-test was used to compare data of two groups. P values less than 0.05 were considered statistically significant.

Results and discussion

Enzymatic cycling assay in capillary

The cycling assay couples the following two enzymatic reactions:

$$Lactate + NAD^+ \xrightarrow{Lactate\ dehydrogenase} Pyruvate + NADH$$

$$NADH + Resazurin \xrightarrow{Daiphorase} NAD^+ + Resorufin$$

NAD^+ and NADH serves as the mediator of the coupling.

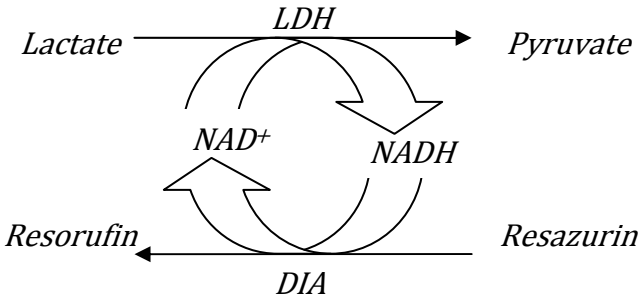

To establish the independent assay of NAD^+ and NADH in a single run, the electrophoretic behavior of all reagents, including both enzymes, was first evaluated. It

was found that 100mM Tris buffer at pH8.5 can separate all six components. Their relative electrophoretic mobility is shown in Figure 4. NADH has the slowest migration rate while NAD^+ has the highest migration rate except lactate, which migrates much faster than the others. For NAD^+ and NADH, this means: 1) they can be separately quantified after electrophoresis separation under this condition; 2) a proper separation time or distance needs to be established to ensure the contact with all the other five chemicals for both NAD^+ and NADH. The scheme for the detection of both NAD^+ and NADH was shown in Figure 5; 3 min separation was sufficient to separate NAD^+ and NADH, so they can mediate enzymatic cycling assay at two different locations in the capillary (Figure 6).

Detection limit and dynamic range of the online cycling method

The enzymatic assay used in this study produces a fluorescent product, resorufin. This makes it possible to carry out the enzymatic cycling reaction in a capillary and detect the product with laser-induced-fluorescence (LIF) to achieve low detection limit.

Besides incubation time and enzyme concentration (both LDH and DIA), the concentration of substrate resazurin has a great effect on detection sensitivity. At the detection wavelength used (~580nm), resazurin is weakly fluorescent. Although a higher concentration of resazurin gives faster reaction, it also means higher background and noise. Additionally, under current experimental conditions, NADH peak is very close to the system peak. With a running buffer containing 0.2 U/mL LDH, 0.2 U/mL DIA, 0.5 mM lactate and 0.25 μM resazurin, the detection limit of NAD^+ can reach down to 0.2 nM of NADH and 1 nM of NAD^+, which corresponds to 0.2 amol and 1 amol respectively. However, the low level of resazurin used in this experimental condition

limits the dynamic range of the system only up to 200 nM NAD^+ and NADH. To determine the relatively high level of NAD^+ and NADH in mammalian cells, 1.5 μM resazurin is used in the running buffer, with which up to 1 μM NAD^+ and NADH can be quantified (Figure 7). The detection limits for both species, however, are compromised under this condition.

Reproducibility of the method

To assess the reproducibility of the on-capillary enzymatic cycling assay, 500 nM NAD^+ was run 6 times, with 0, 100, 200, 500, 800, 1000 nM NADH; the relative standard deviation (RSD) of the peak height is 0.040. Similarly, 500 nM NADH was also run 6 times with 0, 100, 200, 500, 800, 1000 nM NAD^+ and the RSD of the peak height is 0.050.

Specificity of the method

Five NAD(H) related compounds listed in Table 1, which are also present in cells, are tested using the same assay. 1 μM of each compound is tested and none was found to be nearly as effective as NAD^+ or NADH in mediate this enzymatic cycling reaction.

Cell viability

For cell lines, cell viability was higher than 90% under normal condition and there is no significant decrease (< 5%) under treatment with H_2O_2 or 3-aminobenzamide followed by H_2O_2. Primary astrocyte culture has a lower viability even without treatment, around 80%. Exposure to H_2O_2 does not increase the death rate.

Reliability of single-cell assay

Since no obvious morphological change was observed with Tesla coil lysing, conventional extraction method was used to verify whether the in-capillary release of

NAD^+ and NADH is complete. NAD^+ and NADH contents of a single H9c2 cell under normal condition determined by the single-cell assay agree with those obtained from cell extracts. Table 2 shows that there is no significant difference between the two methods. The cellular amount of NAD^+ and NADH determined here is also in the same range with reported data[36]. As with bulk exaction, this method neither differentiates NAD^+ or NADH from different sub-cellular compartments, nor those binded from free ones.

Single cell analysis

The size of H9c2 cells varies from 10 μm to 40 μm in diameter. The cells picked for analysis are all around 20 μm. The electropherogram of a single H9c2 cell is shown in Figure 8. NAD^+ and NADH content of 8 cells under normal condition, 6 cells treated with H_2O_2, and 7 cells treated with 3-aminobenzamide followed by H_2O_2 is shown in Figure 9. Significant variances within each group can be observed. Between groups, H9c2 cell under normal condition contains in average 780×10^{-18} mole NAD^+ and 110×10^{-18} mole NADH; NAD^+ level in cells exposed to 100 μM H_2O_2 for 1 hour decreased to 420×10^{-18} mole and NADH decreased to 40×10^{-18} mole; cells treated with 3-aminobenzamide and H_2O_2 remain NAD^+ level similar to that of normal cells ($P > 0.1$), with in average 670×10^{-18} mole NAD^+ and 4×10^{-18} mole NADH per cell. The NADH/NAD^+ ratio decreases from 0.15 under normal condition to 0.11 under H_2O_2, to 0.006 under H_2O_2 treatment with 3-aminobenzamide.

The trends of NAD^+ level change under H_2O_2 stress and with PARPs inhibitor agree with Gilad et al.'s study of myocardial oxidant injury to the same cell line by H_2O_2 [8]. Apparently, H_2O_2 causes DNA damage in H9c2 cells; PARPs are activated and consume intracellular NAD^+ to repair DNA. NADH is also reduced probably because

part of it is converted to NAD^+. While the 3-aminobenzamide inhibits PARPs function and stops NAD^+ depletion, H_2O_2 still induce DNA damage, resulting in intracellular NADH reduction and NADH/NAD^+ ratio decline. Whether a part of NAD^+ is converted to NADH is not known.

The size of astrocytes varies more than that of H9c2 cells; it is no surprise that NAD^+ and NADH level in astrocytes varies significantly (Table 3). Unlike H9c2 cells, the ratio of NADH/NAD^+ in astrocytes increases under H_2O_2 treatment (Figure 10). This implies that astrocytes respond to H_2O_2 stress following a different mechanism than H9c2 cells.

CONLUSION

We have developed a new method to quantify coenzymes NAD^+ and NADH by coupling an enzymatic cycling reaction with CE-LIF. This method is capable of separating and determining NAD^+ and NADH from a single cell in a single run. Detection limit of NAD^+ and NADH can reach down to 0.2 amol and 1 amol, respectively; the assay can measure NAD^+ and NADH up to 1 μM with higher concentration of resazurin in the reaction buffer. If other reactions can be incorporated into the same reaction buffer (e.g., converting $NADP^+$ to NADPH in the presence of glucose-6-phosphate and G6P dehydrogenase), other intracellular species such as $NADP^+$ and NADPH may also be separated and determined.

A parameter more interesting than the total amount of cellular NAD^+ and NADH is the amount of each nucleotide confined in different cell compartments such as cytosol or mitochondria. Free NADH (in contrast with NADH bound to protein) has also been

intriguing because it is directly correlated with many cellular reaction constants, but its quantification has been extremely difficult. If a gentler cell lysing process, which break down not the whole cell but only specific cellular compartments or does not disturb the binding of NADH to proteins, can be coupled with the CE-based assay in this work, compartmentalized NAD^+, NADH and free NADH would be determined.

Based on results of this study, 1 hour incubation with 100 μM H_2O_2 reduced both NAD^+ and NADH level in H9c2 cells. This change might be due to the activation of poly(ADP-ribose) polymerases in response to DNA damage, since the application of PARPs inhibitor, 3-aminobenzamide, prevent the reduction of NAD^+. It indicates that this dosage of H_2O_2 and exposure time has been severe enough to cause DNA strand breakage and cellular NAD^+ depletion; NADH, which is in equilibrium with NAD^+, is reduced during the long incubation period correspondingly. The NADH/NAD^+ ratio declines significantly in cells treated with 3-aminobenzamide followed H_2O_2, while NAD^+ level is almost unchanged.

The same oxidative stress induces different response in primary astrocyte culture: the intracellular NADH/NAD^+ ratio increases to resist oxidative damage. Why different cells react to the same stimulus differently and the mechanism involved is a matter of interest.

Acknowledgement

E.S.Y. thanks the Robert Allen Wright Endowment for Excellence for support. We thank Professor Srdija Jeftinija of Department of Biomedical Sciences at Iowa State University for providing the astrocyte primary culture. The Ames Laboratory is operated

for the U.S. Department of Energy by Iowa State University under Contract No. W-7405-Eng-82. This work was supported by the Director of Science, Office of Basic Energy Sciences, Division of Chemical Sciences.

References

(1) Li, N.; Chen, G. *Talanta* **2002**, *57*, 961-967.

(2) Ying, W. *Frontiers in Bioscience* **2007**, *12*, 1863-1888.

(3) Belenky, P.; Bogan, K. L.; Brenner, C. *Trends Biochem. Sci.* **2007**, *32*, 12-19.

(4) Lin, S. J.; Guarente, L. *Curr. Opin. Cell Biol.* **2003**, *15*, 241-246.

(5) Hwang, K. C.; Jeong, D. W.; Lee, J. W.; Kim, I. H.; Chang, H. I.; Kim, H. J.; Kim, I. Y. *Mol. Cells* **1999**, *9*, 429-435.

(6) Liang, J.; Wu, W.-L.; Liu, Z.-H.; Mei, Y.-J.; Cai, R.-X.; Shen, P. *Spectrochim. Acta, Part A* **2007**, *67A*, 355-359.

(7) Hudak, B. B.; Tufariello, J.; Sokolowski, J.; Maloney, C.; Holm, B. A. *Am. J. Physiol-lung C.* **1995**, *13*, L59-L64.

(8) Gilad, E.; Zingarelli, B.; Salzman, A. L.; Szabo, C. *J. Mol. Cell. Cardiol.* **1997**, *29*, 2585-2597.

(9) Alano, C. C.; Ying, W. H.; Swanson, R. A. *J. Biol. Chem.* **2004**, *279*, 18895-18902.

(10) Szabo, C.; Dawson, V. L. *Trends Pharmacol. Sci.* **1998**, *19*, 287-298.

(11) Payot, S.; Guedon, E.; Gelhaye, E.; Petitdemange, H. *Res. Microbiol.* **1999**, *150*, 465-473.

(12) Zerez, C. R.; Lachant, N. A.; Tanaka, K. R. *Blood* **1990**, *76*, 1008-1014.

(13) Zhang, Q. H.; Wang, S. Y.; Nottke, A. C.; Rocheleau, J. V.; Piston, D. W.; Goodman, R. H. *Proc. Natl. Acad. Sci. U. S. A.* **2006**, *103*, 9029-9033.

(14) Lohmann, W.; Mussmann, J.; Lohmann, C.; Kunzel, W. *European Journal of Obstetrics Gynecology and Reproductive Biology* **1989**, *31*, 249-253.

(15) Pogue, B. W.; Pitts, J. D.; Mycek, M. A.; Sloboda, R. D.; Wilmot, C. M.; Brandsema, J. F.; O'Hara, J. A. *Photochem. Photobiol.* **2001**, *74*, 817-824.

(16) Jones, D. P. *J. Chromatogr., B: Anal. Technol. Biomed. Life Sci.* **1981**, *225*, 446-449.

(17) Ryll, T.; Wagner, R. *J. Chromatogr., B: Anal. Technol. Biomed. Life Sci.* **1991**, *570*, 77-88.

(18) Litt, M. R.; Potter, J. J.; Mezey, E.; Mitchell, M. C. *Anal. Biochem.* **1989**, *179*, 34-36.

(19) Yamada, K.; Hara, N.; Shibata, T.; Osago, H.; Tsuchiya, M. *Anal. Biochem.* **2006**, *352*, 282-285.

(20) Lowry, O. H.; Rock, M. K.; Schulz, D. W.; Passonneau, J. V. *J. Biol. Chem.* **1961**, *236*, 2746-2755.

(21) Zerez, C. R.; Lee, S. J.; Tanaka, K. R. *Anal. Biochem.* **1987**, *164*, 367-373.

(22) Ying, W. H.; Garnier, P.; Swanson, R. A. *Biochem. Biophys. Res. Commun.* **2003**, *308*, 809-813.

(23) Cook, D. B.; Self, C. H. *Clin. Chem.* **1993**, *39*, 965-971.

(24) Dekoning, W.; Vandam, K. *Anal. Biochem.* **1992**, *204*, 118-123.

(25) Graeff, R.; Lee, H. C. *Biochem. J.* **2002**, *361*, 379-384.

(26) Bembenek, M. E.; Kuhn, E.; Mallender, W. D.; Pullen, L.; Li, P.; Parsons, T. *Assay Drug Dev. Technol.* **2005**, *3*, 533-541.

(27) Wang, Z. Q.; Yeung, E. S. *J. Chromatogr., B: Anal. Technol. Biomed. Life Sci.* **1997**, *695*, 59-65.

(28) Huang, W.-H.; Ai, F.; Wang, Z.-L.; Cheng, J.-K. *J. Chromatogr., B: Anal. Technol. Biomed. Life Sci.* **2008**, *866*, 104-122.

(29) Piston, D. W.; Masters, B. R.; Webb, W. W. *Journal of Microscopy-Oxford* **1995**, *178*, 20-27.

(30) Pitts, J. D.; Sloboda, R. D.; Dragnev, K. H.; Dmitrovsky, E.; Mycek, M. A. *Journal of Biomedical Optics* **2001**, *6*, 31-40.

(31) Konig, K.; So, P. T. C.; Mantulin, W. W.; Tromberg, B. J.; Gratton, E. *Journal of Microscopy-Oxford* **1996**, *183*, 197-204.

(32) Kasischke, K. A.; Vishwasrao, H. D.; Fisher, P. J.; Zipfel, W. R.; Webb, W. W. *Science (Washington, DC, U. S.)* **2004**, *305*, 99-103.

(33) Ramanujan, V. K.; Zhang, J. H.; Biener, E.; Herman, B. *Journal of Biomedical Optics* **2005**, *10*.

(34) Hogan, B. L.; Yeung, E. S. *Anal. Chem.* **1992**, *64*, 2841-2845.

(35) Lee, T. T.; Yeung, E. S. *Anal. Chem.* **1992**, *64*, 3045-3051.

(36) Xue, Q.; Yeung, E. S. *J. Chromatogr., A* **1994**, *661*, 287-295.

(37) Xue, Q.; Yeung, E. S. *J. Chromatogr., B: Anal. Technol. Biomed. Life Sci.* **1996**, *677*, 233-240.

(38) Bergquist, J.; Tarkowski, A.; Ekman, R.; Ewing, A. *Proc. Natl. Acad. Sci. U. S. A.* **1994**, *91*, 12912-12916.

(39) Xue, G.; Pang, H. M.; Yeung, E. S. *J. Chromatogr., A* **2001**, *914*, 245-256.

(40) Chang, H. T.; Yeung, E. S. *Anal. Chem.* **1993**, *65*, 2947-2951.

(41) Ma, Y.; Shortreed, M. R.; Li, H.; Huang, W.; Yeung, E. S. *Electrophoresis* **2001**, *22*, 421-426.

(42) Bao, J.; Regnier, F. E. *J. Chromatogr., A* **1992**, *608*, 217-224.

(43) Arcibal, I. G.; Santillo, M. F.; Ewing, A. G. *Anal. Bioanal. Chem.* **2007**, *387*, 51-57.

Table 1. Response of possible interference by NAD(H) related compounds.

Compound (1μM)	Response relative to NAD^+	Response relative to NADH
Nicotinamide adenine dinucleotide (NAD^+)	100	---
Nicotinamide adenine dinucleotide phosphate ($NADP^+$)	---	100
Nicotinic acid adenine dinucleotide (NAAD)	0.2	0
Nicotinic acid adenine dinucleotide (NAAD)	0.3	0
Nicotinamide mononucleotide (NMN)	<0.1	0
Nicotinic acid (NA)	<0.1	0
Nicotinamide (NAM)	<0.1	0

Table 2. Amount of NAD^+ and NADH in a single H9c2 cell under normal condition

NAD^+/amol		NADH/amol	
single cell analysis	cell extract analysis	single cell analysis	cell extract analysis
775 ± 84	726 ± 117	111 ± 60	108 ± 8

Table 3. NAD^+ and NADH amount in single astrocytes

UNDER NORMAL CONDITION				UNDER H_2O_2			
	NAD^+/amol	NADH/amol	NADH/NAD^+		NAD^+/amol	NADH/amol	NADH/NAD^+
Cell 1	266.08	69.66	0.2618	Cell 1	209.99	104.25	0.4965
Cell 2	180.78	60.11	0.3325	Cell 2	333.20	127.41	0.3824
Cell 3	248.78	49.78	0.2001	Cell 3	234.20	185.19	0.7908

Figure captions

Figure 1 Diagram of the home-made capillary electrophoresis system.

Figure 2 Photograph of the injection end of home-made capillary electrophoresis setup.

Figure 3 Illustration of single cell lysing in capillary with Tesla coil.

Figure 4 Electrophoregrams of the 6 components of the enzymatic cycling reaction in Tris buffer (100 mM, pH 8.5) on a Beckman P/ACE™ system.

Figure 5 Separation and detection of 500 nM NAD^+ and 500 nM NADH.

Figure 6 Scheme of the on-capillary enzymatic cycling assay for detecting of NAD^+ and NADH.

Figure7 Fitting curves for NAD^+ detection (A) and NADH detection (B). The running buffer contains 0.5 mM lactate, 1.5 uM resazurin, 0.1U/mL LDH and 0.1 U/mL DIA, all in 100 mM Tris buffer (pH 8.5).

Figure 8 Electrophoregram of a single normal H9c2 cell analyzed by the enzymatic cycling assay.

Figure 9 Single cell analysis results of (A) NAD^+; (B) NADH; (C) NADH/NAD^+ ratio of single H9c2 cells.

Figure 10 Cellular NADH/NAD^+ ratio of normal astrocytes and astrocytes treated with H_2O_2.

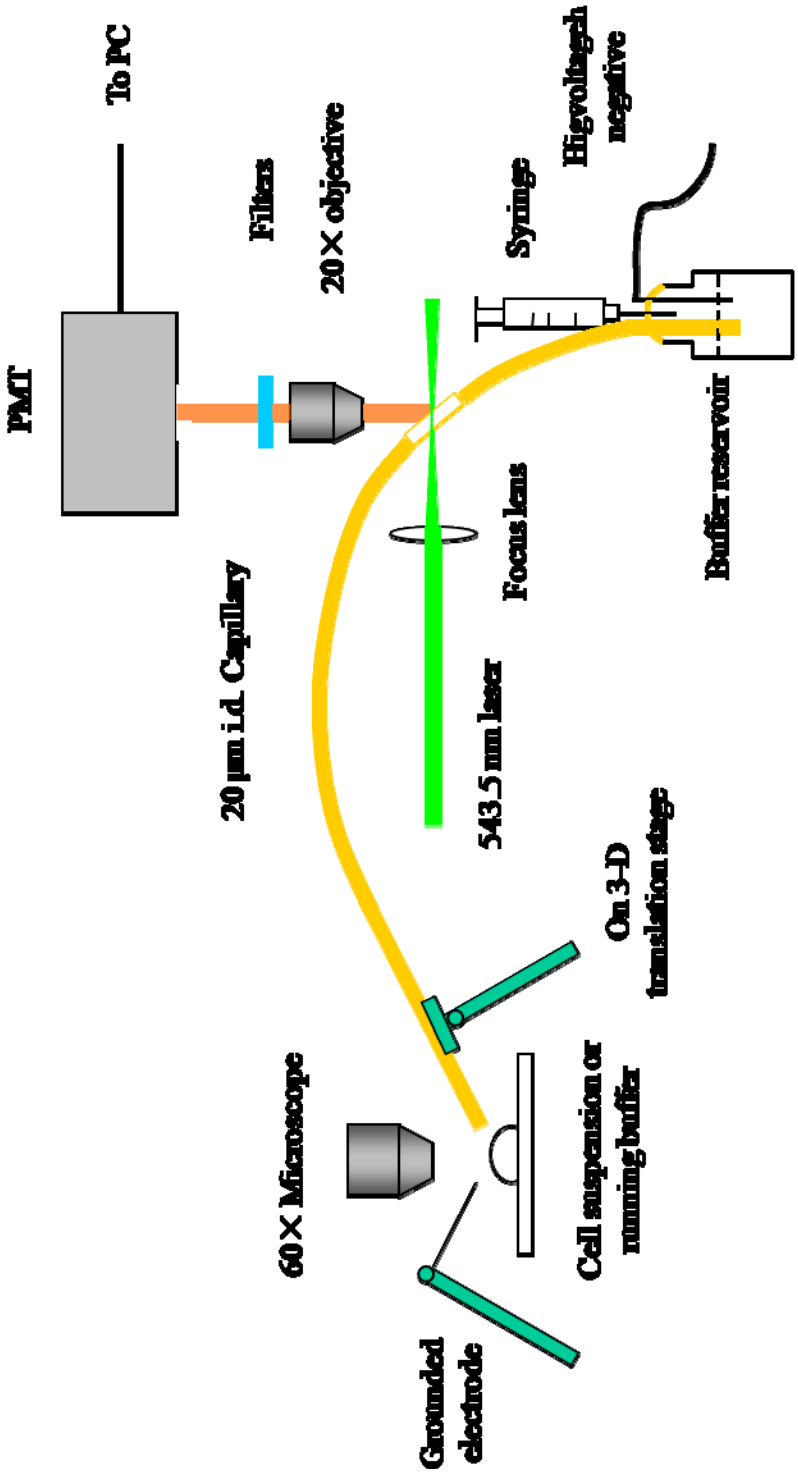
To PC
Filters
20× objective
Syringe
Higvoltage negative
PMT
20 µm i.d. Capillary
Focus lens
Buffer reservoir
543.5 nm laser
On 3-D translation stage
60× Microscope
Cell suspension or running buffer
Grounded electrode

Figure1

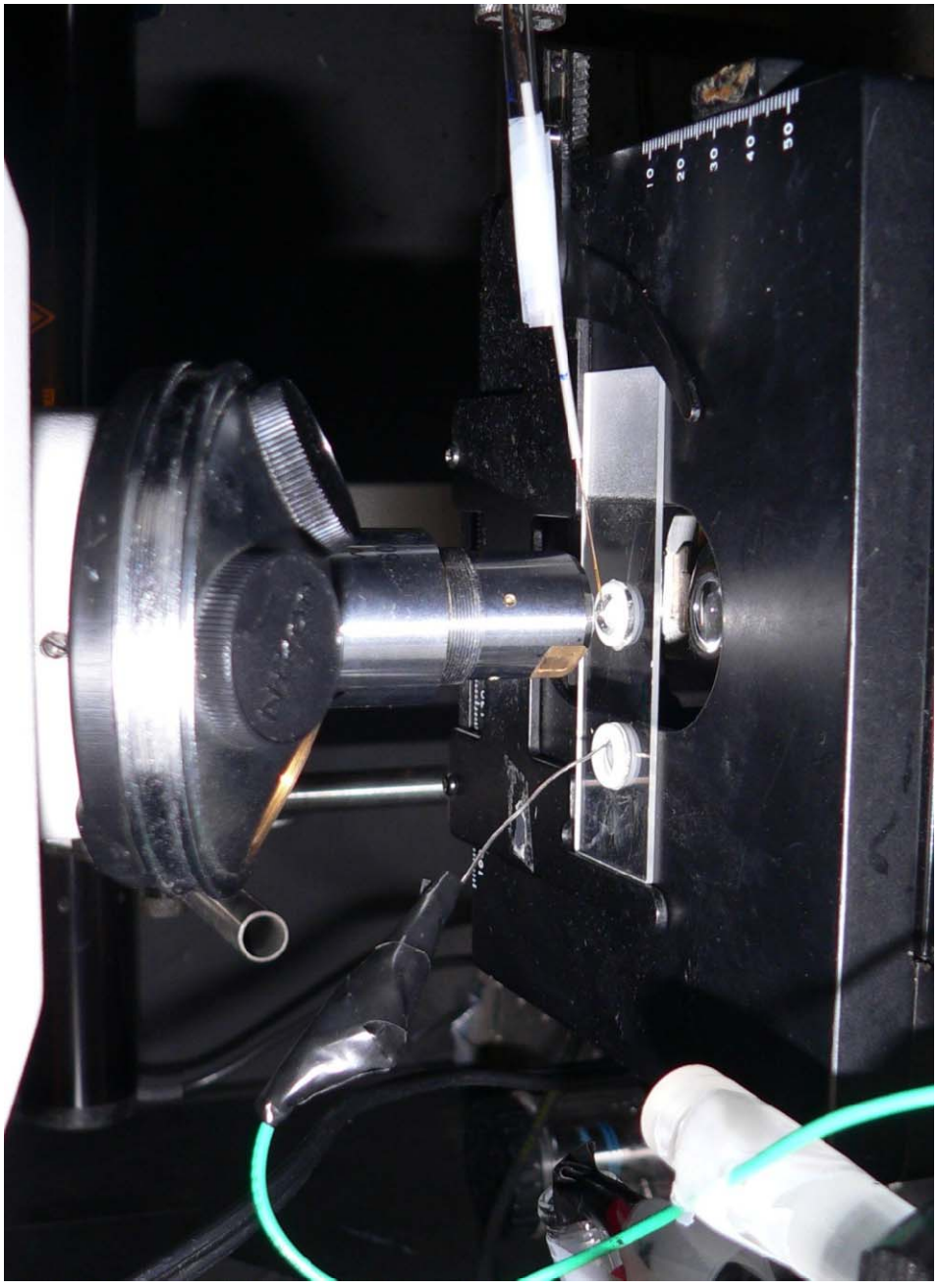

Figure2

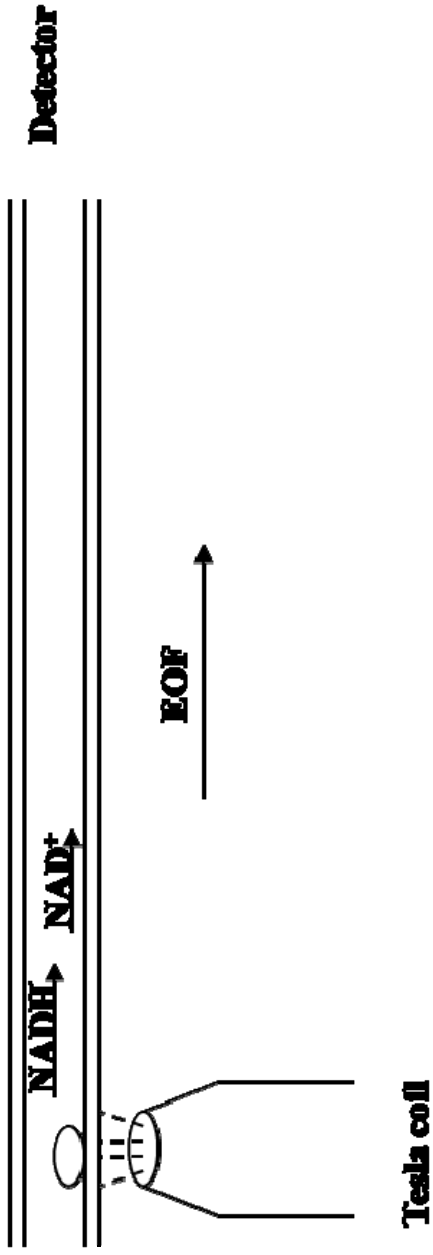

Figure3

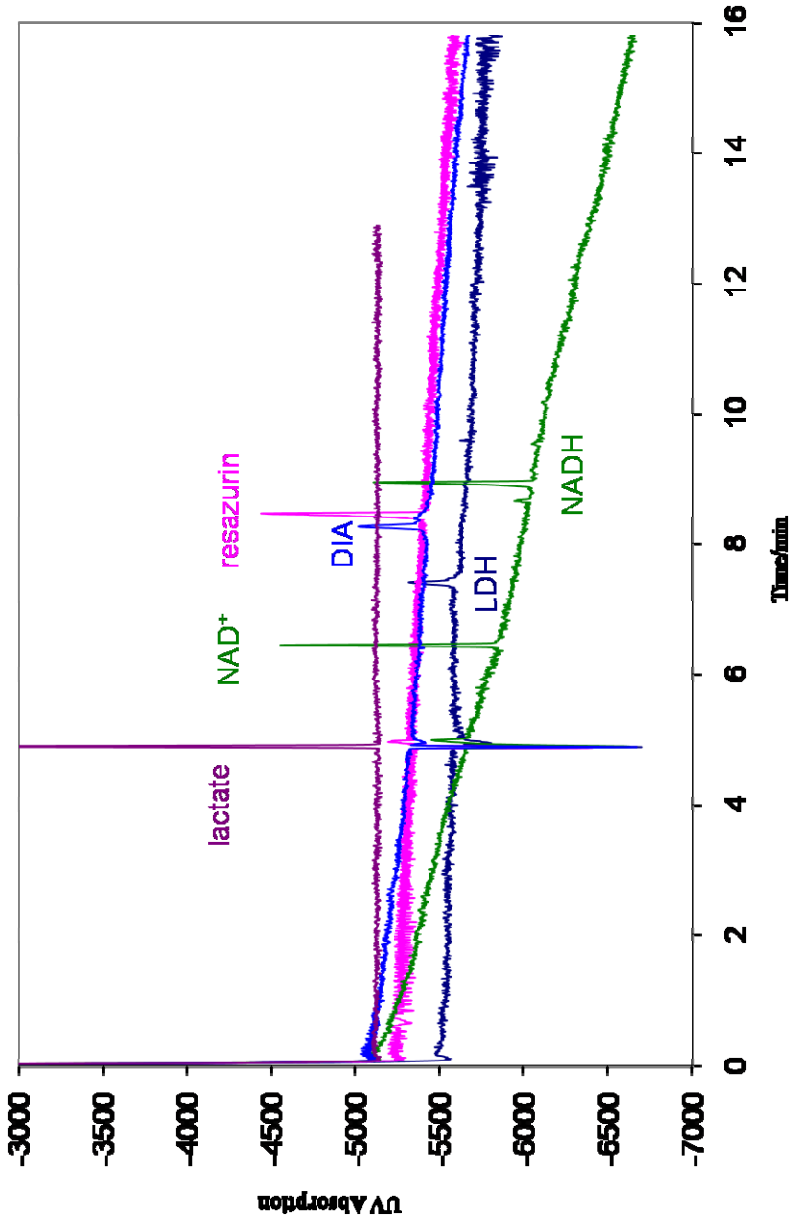
-3000
-3500
-4000
-4500
-5000
-5500
-6000
-6500
-7000
UV Absorption
0
2
4
6
8
10
12
14
16
Time/min
lactate
NAD+
resazurin
DIA
LDH
NADH

Figure4

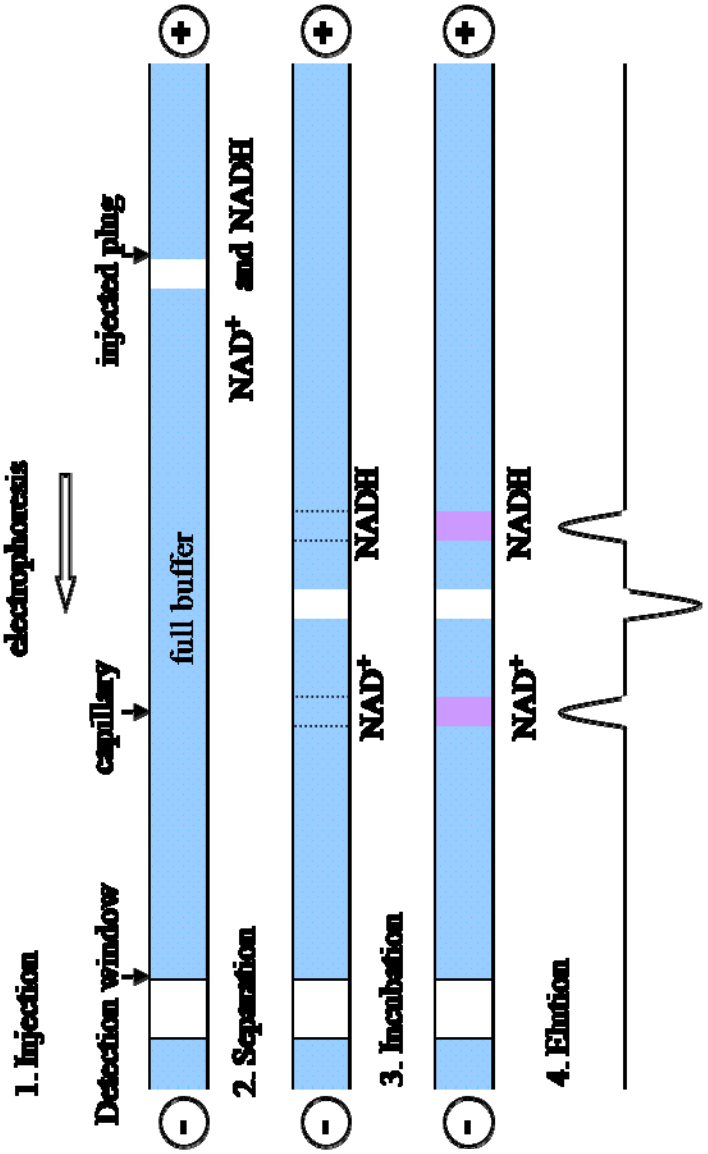
1. Injection
Detection window
capillary
electrophoresis
injected plug
full buffer
NAD+ and NADH
2. Separation
NAD+
NADH
3. Incubation
NAD+
NADH
4. Elution
-
+

Figure 5

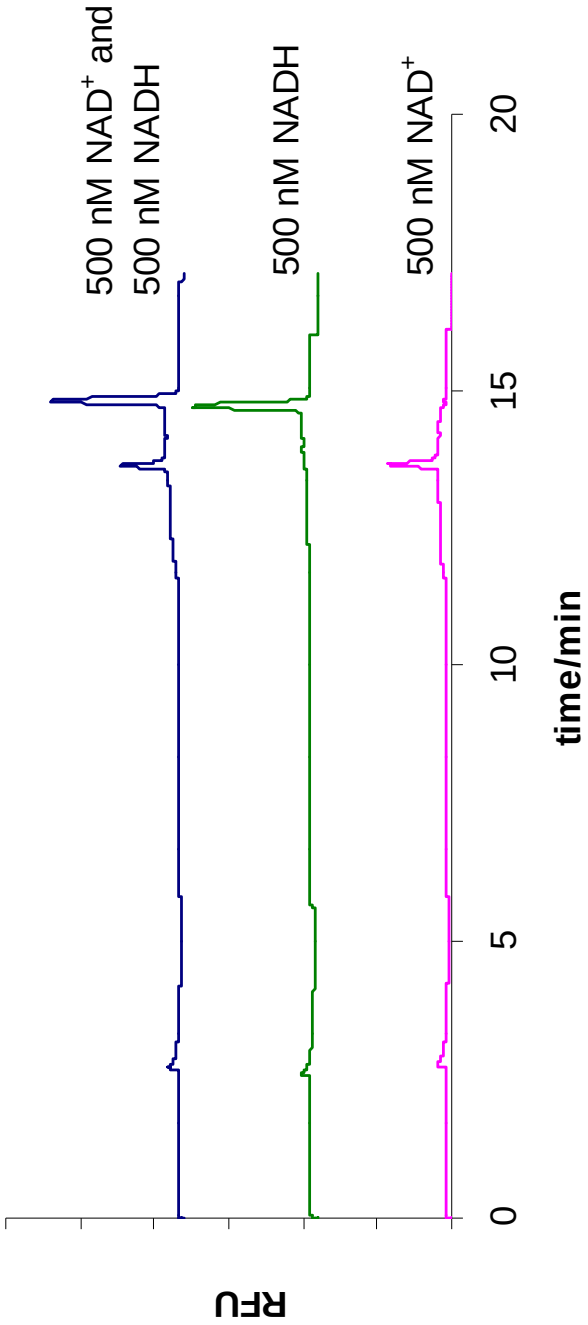
500 nM NAD+ and
500 nM NADH
500 nM NADH
500 nM NAD+
RFU
0
5
10
15
20
time/min

Figure 6

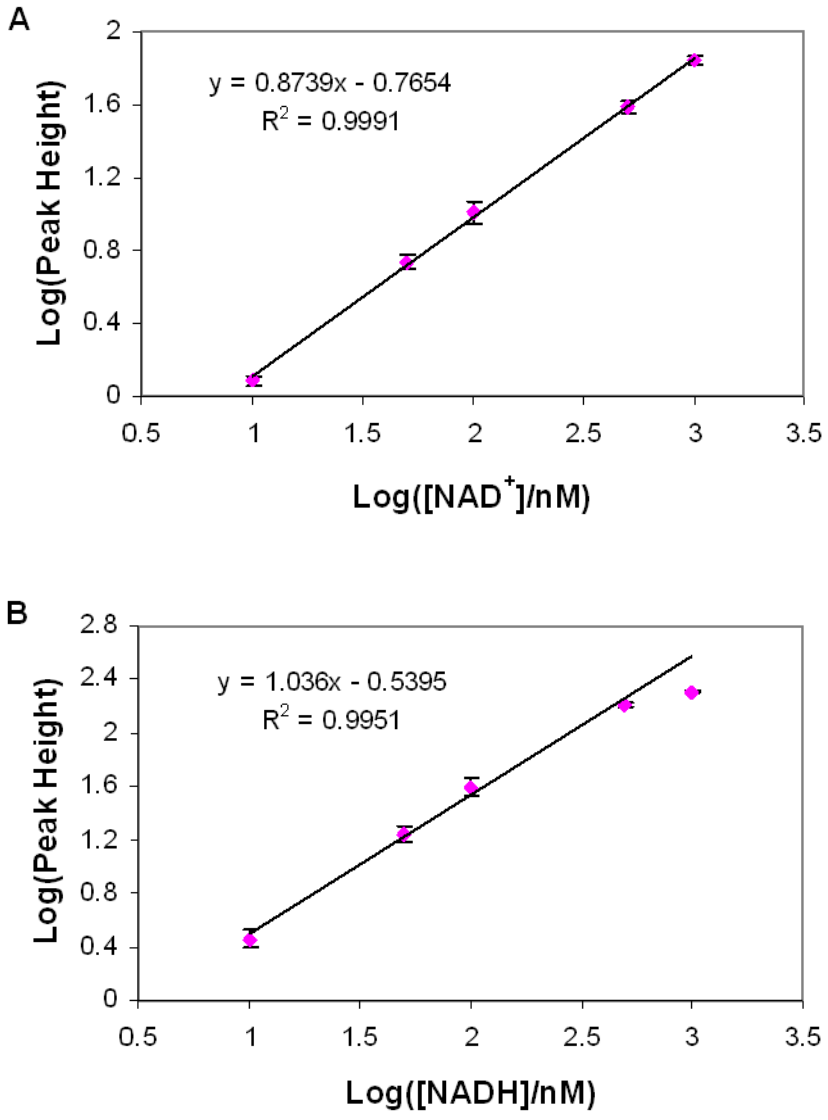
A
y = 0.8739x - 0.7654
R2 = 0.9991
Log(Peak Height)
Log([NAD+]/nM)
B
y = 1.036x - 0.5395
R2 = 0.9951
Log(Peak Height)
Log([NADH]/nM)

Figure 7

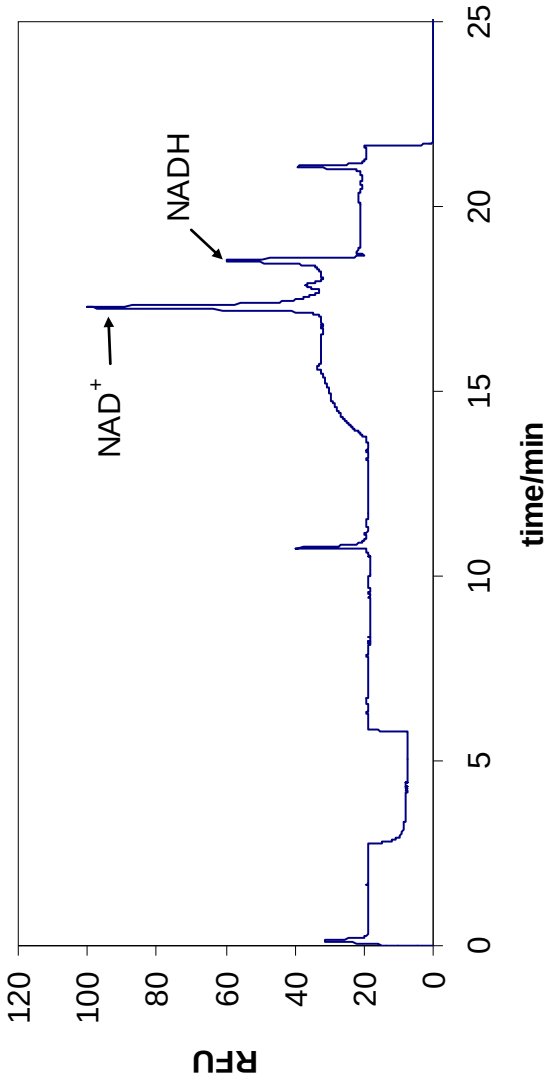

Figure 8

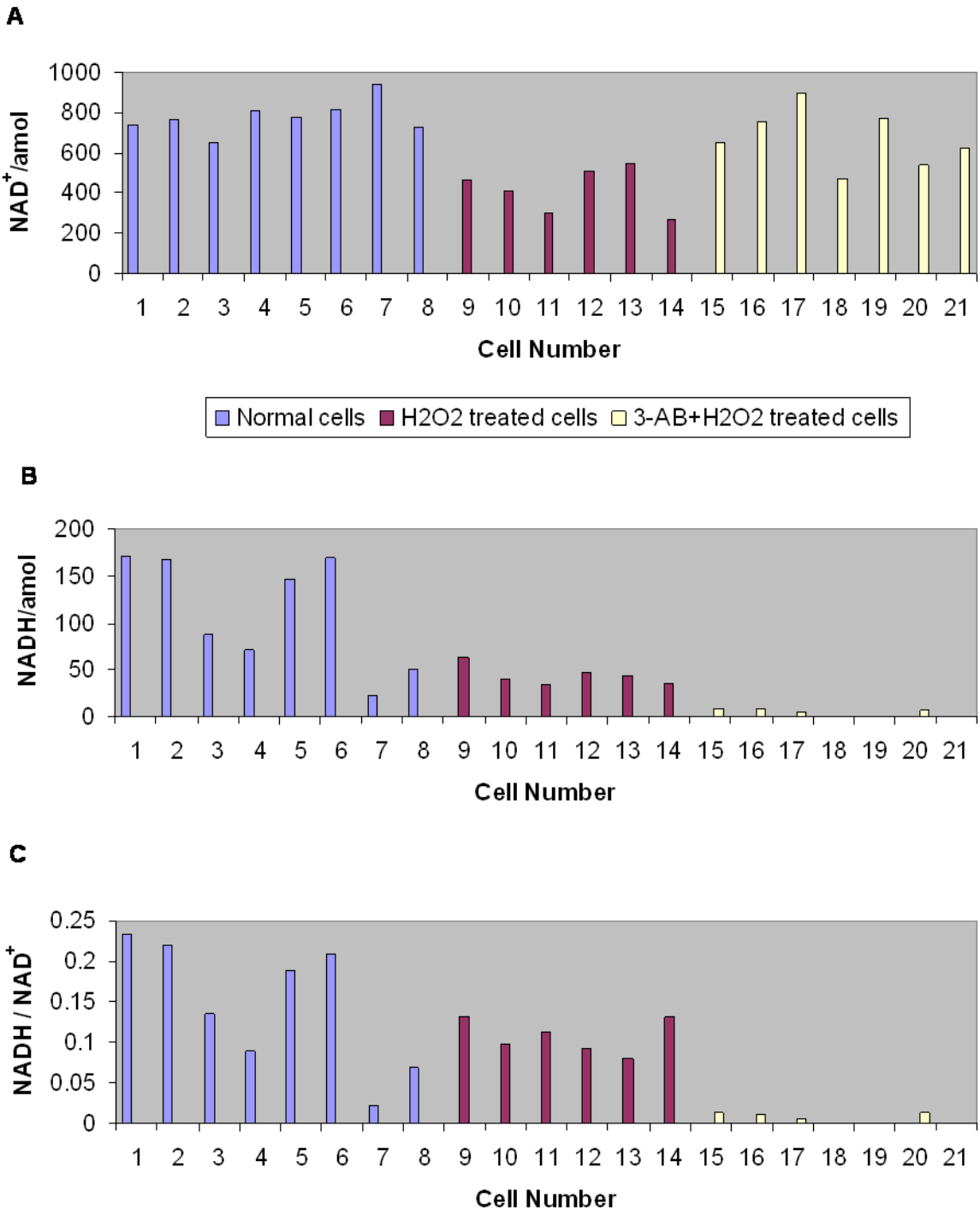
A
NAD+/amol
1000
800
600
400
200
0
1 2 3 4 5 6 7 8 9 10 11 12 13 14 15 16 17 18 19 20 21
Cell Number
Normal cells
H2O2 treated cells
3-AB+H2O2 treated cells
B
NADH/amol
200
150
100
50
0
1 2 3 4 5 6 7 8 9 10 11 12 13 14 15 16 17 18 19 20 21
Cell Number
C
NADH / NAD+
0.25
0.2
0.15
0.1
0.05
0
1 2 3 4 5 6 7 8 9 10 11 12 13 14 15 16 17 18 19 20 21
Cell Number

Figure 9

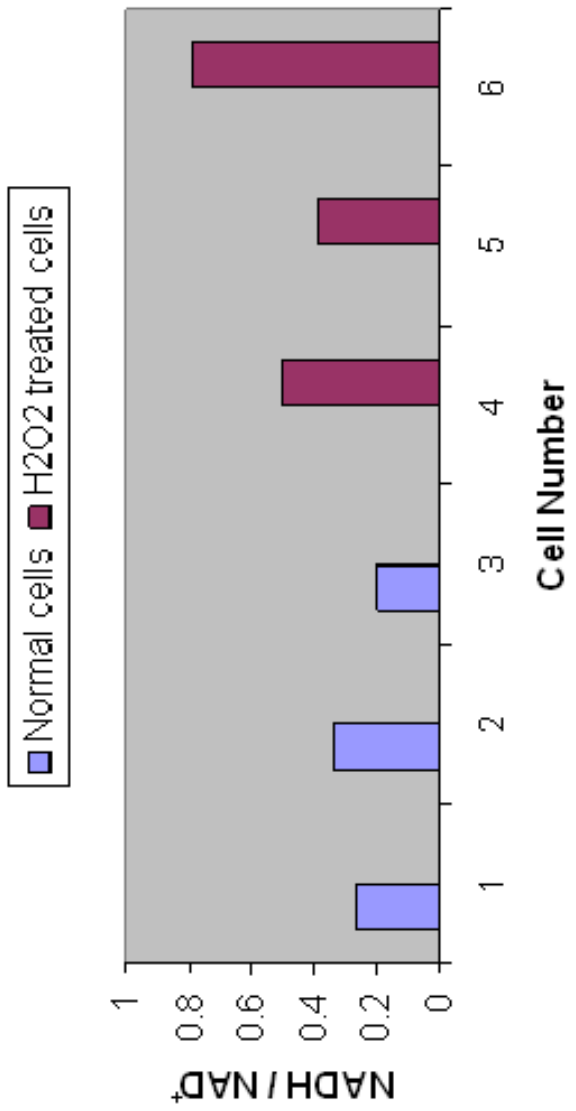
Normal cells
H2O2 treated cells
NADH / NAD+
0
0.2
0.4
0.6
0.8
1
1
2
3
4
5
6
Cell Number

Figure10

CHAPTER 4. CAPILLARY ELECTROPHORETIC ASSAY OF SINGLE ENZYME CRYSTALS

A paper prepared for submission to Analytical Chemistry

Aoshuang Xu, Fenglei Li, Wei Wei, and Edward S. Yeung

Abstract

Human lactate dehydrogenase isozyme 1 (LDH) crystals were separately dissolved and subsequently assayed inside capillaries with electrophoretically mediated microanalysis (EMMA). Crystal LDH activities were compared at both ensemble and single molecule level. Plug-plug mode EMMA with UV absorption detection was used to compare the average activity among crystals and among the fragments of single crystals. While fragments from the same crystal exhibited identical enzyme activity, different crystals grown from the same crystallization condition showed markedly different activity. A total of 21 crystals obtained from similar crystallization condition clearly showed discrete activity levels. Continuous mode EMMA with laser induced fluorescence was employed to study crystals of LDH at the single molecule level. Activities of LDH molecules from a crystal are essentially identical within experimental error, where as LDH molecules directly from solution shows about four-fold variation in activity. Furthermore, after storage at 37 °C, activity distribution of LDH molecules broadens and resembles that of LDH directly from solution. These results correlate well with previous X-ray crystallography data and support the hypothesis that the slow equilibrium of multiple

conformations of LDH in solution contributes significantly, if not solely, to the observed single molecule activity heterogeneity.

Introduction

Enzymes are biomolecules that catalyze chemical reactions. Almost all enzymes are proteins and the enzyme catalytic activity is ultimately determined by the folded three-dimensional structure of the polypeptide[1]. Traditional enzymology studies enzyme activity at the ensemble level with bulk aqueous solution, describing the average catalytic behavior of enzyme molecules. Recent studies at single enzyme level reveal considerable molecule-to-molecule variation in terms of catalytic activity[2-16]. Furthermore, experiments following the reaction trajectories of single enzyme molecules show that the enzymatic reaction rate is constantly fluctuating[8-13, 15]. These two phenomena of enzyme activity, known as the static and dynamic heterogeneity, respectively, reflect the molecule-to-molecule structural variation and molecular structural dynamic of enzymes.

The inherent complexity of proteins gives enzyme molecules many structural degrees of freedom, leading to a rugged free energy landscape and possible multiple conformational states at local energy minima[17]. A fluctuating enzyme model where multiple enzymatic conformations interconvert on the time scale of catalytic activity was proposed[8] to explain the observed dynamic heterogeneity in enzymatic activity and supported by conformational dynamics probed by electron transfer[18-20], florescence resonance energy transfer[10, 21], and NMR[22] experiments.

Although conformational dynamics satisfactorily explains enzymatic dynamic heterogeneity, caution should be exercised in extending it to static heterogeneity for two reasons. First, static heterogeneity were observed on a much larger time scale, usually tens of thousands

turnover cycles or more, which means much higher energy barriers between conformations and conformations stable over a much longer period. Direct observations of such conformations in solution state so far have been missing. Second, most experiments have been carried out with commercially available or relatively crudely separated enzymes, which may be heterogeneous in their primary sequence, possibly caused by heterogeneous post-translational modifications. In fact, Polakowski et al. showed that while highly purified bacterial alkaline phosphatase has identical activity, endogenous proteolysis results in activity heterogeneity[23]. Other studies on enzymes that show static heterogeneity, however, have not been able to determine whether conformational multiplicity plays a role.

Capillary electrophoresis (CE) is a powerful technique in enzyme activity study and has played an instrumental role in single molecule enzyme study. The principle of enzyme assay with CE was first established in 1992 by Bao et al.[24] and later named as electrophoretically mediated microanalysis (EMMA)[25]. There are some excellent reviews on this topic[26-29]. Briefly, two general assay modes of EMMA can be identified. In plug-plug mode, substrate and enzyme are injected separately and the electrophoretic mobility difference between the two is used to ensure mixing. Reaction occurs at where the mixing is. Incubation without electric field can be used to allow further progress of the assay as needed. In continuous mode, the substrate is included in the background electrolyte buffer. Enzyme sample is injected and swept through the capillary by electrophoresis. Product appears as a plateau as the enzyme sweeps through capillary. Incubation in continuous mode EMMA produces a product peak over the plateau.

A special version of continuous mode EMMA was frequently used in single enzyme study since Xue's original work[2]. A buffer, containing much diluted enzyme solution and

necessary substrate, is filled in a thin capillary, and incubated for some time for products to accumulate before voltage is applied to drive the products through the detector. Because the enzyme concentration is so low, these molecules are a few centimeters apart on average. Local product pools from individual enzyme will not mix by diffusion during the relatively short incubation time and thus detected as individual peaks, whose areas are proportional to the activities of the corresponding enzyme molecules.

Human lactate dehydrogenase isozyme 1 (LDH) is the first enzyme assayed to show static heterogeneity, which was attributed to the presence of several stable conformations[2]. Recent X-ray crystallography studies in our group revealed multiple conformations of LDH from crystals obtained from the sample crystallization mother liquor. The active site loop of any of the four subunits can be in an open conformation, closed conformation, or two conformations[30]. This direct observation and separation of multiple stable conformations of LDH provide the opportunity to fully assess the contribution of conformations to the static heterogeneity. We present here the study of LDH activity from crystal sources by both plug-plug mode EMMA at the ensemble level and continuous mode EMMA at single molecule level.

Experimental section

Chemicals and reagents

Purified human LDH isozyme 1 (LDH) were purchased from Calzyme (San Luis Obispo, CA). Lithium l-lactate, β-Nicotinamide adenine dinucleotide (NAD+) and its reduced disodium salt (NADH), and sodium salicylate were obtained from Sigma (St. Louis, MO). Crystallization

grade Tris(hydroxylmethyl)aminomethane (Tris), Tris hydrochloride, sodium chloride, sodium hydroxide, PEG 400, PEG 4000 were purchased from Hampton Research (Aliso Viejo, CA).

Protein crystallization

Before crystallization, LDH were dialyzed for 36 hours at 4 °C against 10mM TrisHCl, 50mM NaCl (pH 8.1) buffer using the Slide-A-Lyzer® 10,000 nominal cutoff dialysis cassettes from Pierce Biotechnology (Rockford, IL). 5mM NADH was added to the dialyzed protein solution. The proteins were concentrated to ~20mg/mL (based on final solution volume) at 4 °C using 10,000 nominal cutoff Microcon® centrifugal filters from Millipore (Billerica, MA). Hanging drop vapor diffusion method was used to obtain LDH crystals at room temperature. Hanging protein solution droplets were prepared by mixing equal volumes (1μL each) of the concentrated protein solution and corresponding well solution (0.2M TrisHCl and various concentrations of PEG 400 and PEG 4000 at pH 8.1) on siliconized glass cover slides from Hampton Research.

Crystals were obtained at both 35% PEG 400 and 8% PEG 4000 (v/v) and 34% PEG 400 and 8% PEG 4000 solution. For ensemble average experiment, 14 crystals were harvested from four separate crystallization droplets of 35% PEG 400 and 8% PEG 4000 (v/v): two from droplet A, four from droplet B, six from droplet C, and two from droplet D; seven crystals were harvested from 1 crystallization droplet E of 34% PEG 400 and 8% PEG 4000. Crystals were fished out of the crystallization droplets using Mounted CryoLoop (Hampton Research, Aliso Viejo, CA) of the appropriate size, and immediately dissolved in 6μL (hLDH) dissolving buffer (1mM sodium salicylate, 50mM lithium l-lactate, 10mM TrisHCl, pH8.0). Each crystal from droplet D were carefully separated and split into pieces, and three pieces from each crystal were

dissolved and stored separately. For single molecule experiment, 3 crystals were obtained from one droplet F and 1 crystal from droplet G, both droplets of 34% PEG 400 and 8% PEG 4000 (v/v). Crystals were dissolved in 6µl of 20mM TrisHCl, pH9.0 buffer. The integrity of crystals was confirmed by polarization microscope before harvest. Home-made fused silica vials were used as containers for all initial crystal dissolving and also used as sample vials for enzyme average assay. All dissolved crystals were frozen immediately at -80 °C until further manipulation.

Ensemble average enzyme assay

To compare the relative enzyme activity across these crystals, we designed a two-step capillary electrophoresis (CE) based method. All CE experiments were performed on a Beckman Coulter ProteomeLab PA 800 CE instrument (Fullerton, CA) equipped with a UV absorbance detector filtered at 214nm. Untreated capillary with a total length of 60cm (50cm to detection window), 75µm I.D., and 365µm O.D. (Polymicro, Phoenix, AZ) was used throughout the experiment.

The concentration enzyme solutions were first calibrated against the internal standard (1mM sodium salicylate) by hydrodynamic injection at 0.2psi for 30sec. The enzyme solution was then diluted 5-20× with CE running buffer (50mM lithium l-lactate, 10mM TrisHCl, pH8.0) before being injected for plug-plug mode electrophoretically mediated microassay. For every enzyme solution, calibration was repeated twice while assays were repeated three times. Injection sequences for the assay are: 0.1psi, 10sec diluted enzyme solution; 2kV, 99sec buffer; 1kV, 30sec NAD+. Because NAD+ moves faster than LDH under this buffer condition, NADH was generated when NAD+ zone surpassed LDH zone during electrophoresis. Capillary cartridge

was set at 25 °C and sample tray was set at 6 °C throughout the experiments. Original enzyme solutions were kept on ice after calibration runs and 1μL was taken for dilution for each assay run.

Single molecule assay

A home-made CE-LIF instrument was used for single molecule assay. Briefly, 2.5mW of 364nm laser was isolated from a multiline UV laser (I-90, Coherent, CA) with an equilateral dispersing prism and focused with a 15× UV objective into an 11μm I.D. 150μm O.D. fused silica capillary (Polymicro, Phoenix, AZ). Fluorescence was collected at 90° by a 40× objective (Edmund Scientific, CA), through a 364nm longpass filters (Semrock, Rochester, NY) and two bandpass filters (430nm to 630nm and 420nm to 520nm) (Semrock, Rochester, NY), and focused on a side-on photomultiplier tube (PMT) (Model R928, Hamamatsu, Bridgewater, NJ). The analog fluorescence signals collected by the PMT were digitized by a pDaq55 A/D converter (Iotech, Cleveland, OH) and recorded at 10Hz with a home-built Labview program on a PC.

CE buffer contains 20mM TisHCl, 3mM L-lithium lactate, and 1mM NAD+ adjusted at pH9.0 with 1M sodium hydroxide. Untreated capillary with a total length of 55cm (45cm to detection window), 11μm I.D., and 150μm O.D. (Polymicro, Phoenix, AZ) was used throughout the experiment. A 36cm section of the capillary was surrounded with a water bath jacket and temperature-regulated by circulating water. Two bath/circulators were individually maintained at 40 °C and 22 °C. Connections between the bath/circulators and the capillary jacket were achieved by coupling pairs (Colder Products, St. Paul, MN) so that water circulating the capillary jacket could be instantaneously switched between 40 °C and 22 °C.

Enzyme solution was diluted in steps of $10^3\times$ or $10^2\times$ to a certain concentration in 20mM TrisHCl, pH9.0 buffer and stored in ice through the assay. 1μL of the diluted enzyme solution was mixed with 1mL of CE buffer and filled into the capillary electrophoretically at 21kV for 7 minutes with 22 °C circulating water bath. The water bath was then switched to 40 °C for 1 hour incubation. Product zones were driven through the detection window by 21kV voltage with 22 °C circulating water bath. Since the concentration of LDH solution derived from crystals was unknown, usually a few short incubations, starting from the low end of the estimated concentration, were needed to find the proper dilution factor to give single molecule product peaks. Blank runs were performed between actual assays. Standard solution of 2.0×10^{-9}M NADH plug was injected at the beginning of each day to verify the instrument performance and the peak plateau height was used as external calibration for the single enzyme product peaks.

Timing from crystal dissolving, crystal *1* was analyzed on day 3 at -80 °C. Both crystal *2* and *3* were split into two equal portions upon dissolving. The first portion of crystal *2* was analyzed on day 5, and the first portion of crystal *3* was analyzed day 6. The other halves of crystal *2* and *3* were both further split into equal portions upon day 9 and stored half at -80 °C and half at 37 °C. Both portions of crystal *2* were analyzed on day 17 and both portions of crystal 3 were analyzed on day 24. Crystal *4* were split into 4 portions on day 25 and incubated at 37 °C for 0, 12, 24, 48 hours before put at -80 °C again and analyzed on day 28.

Data processing

All integrations were performed in Grams/AI software (Thermo Scientific, Waltham, MA). The relative activity of LDH from ensemble average assay was reported as the area ratio of NADH peak to LDH peak that was calibrated against the internal standard. The relative activity

from single molecule experiment was reported as the area of NADH product peaks corrected for day-to-day variation by NADH external standards. All statistic analysis was done with SigmaPlot (Systat Software, San Jose, CA).

Results and discussion

LDH crystals

Crystals were obtained at both 35% PEG 400 and 8% PEG 4000 (v/v) and 34% PEG 400 and 8% PEG 4000 solution. The sizes of crystals range from 10 to 150nm in any dimension. For ensemble average experiment, 14 crystals were harvested from four separate crystallization droplets of 35% PEG 400 and 8% PEG 4000 (v/v): two from droplet A, four from droplet B, six from droplet C, and two from droplet D; seven crystals were harvested from 1 crystallization droplet E of 34% PEG 400 and 8% PEG 4000. Not all the crystals from the aforementioned droplets were harvested as the droplet dried up quickly once exposed to air.

Assay of LDH from crystals

LDH catalyzes the following reversible reaction:

$$Lactate + NAD^+ \overset{LDH}{\Longleftrightarrow} Pyruvate + NADH$$

Provided with large excess of substrates, the enzyme reactions are linear and the rate of the generation of products or that of the destruction of reagents is proportional to the total activity of the LDH used in the assay. NADH is commonly monitored because of its distinct spectra, namely its absorption around 340nm and fluorescence emission around 460nm. For single molecule assay, high detection sensitivity is required due to limited amount of NADH product from individual enzyme molecule. The forward direction is chosen to use direct

detection with laser induced fluorescence. Direct comparison of enzyme activity can be made by comparing individual enzymatic product peaks as the underlying enzyme quantity is one molecule. For ensemble assay, the same forward reaction is used. However, comparison of activity cannot be made unless the enzyme amount is calibrated due to crystal size variation. Furthermore, the small amount of LDH from each crystal, estimated to be <500ng, also necessitates experiments that demand minimum sample and sample manipulation.

Development of ensemble average enzyme assay with plug-plug mode EMMA

An EMMA method with UV absorption detection at 214nm was developed for comparing ensemble average activities of LDHs of different crystal sources. A plug of LDH solution was injected first, followed by a plug of running buffer and then a plug of NAD+ solution. Because NAD+ migrates faster than LDH, the NAD+ zone catches up and passes LDH zone before reaching the detector. With lactate present in the background electrolytes, NADH is generated upon contact of NAD+ and LDH.

This assay strategy has several advantages. First, to avoid possible enzyme change after dissolving, it is necessary to minimize manipulation of the enzyme after dissolving. Capillary electrophoresis directly samples the enzyme solution and calibrates its concentration with a UV absorption detector. Second, electrophoresis provides a small sampling volume and a small volume reagents mixing scheme so that only a few nanoliter of enzyme solution is used in each assay and multiple replica runs can be carried out to evaluate the assay precision. Third, electrophoresis affords the separation of NAD+, NADH, and LDH so that they can be individually quantified with a single UV absorption detector.

Ideally, both NADH and LDH would be quantified in a single electrophoresis run. However, the catalytic efficiency of LDH is so high (~300U/mg) that a reasonable LDH concentration that can be reliably quantified by the UV detector is too large to maintain linear enzymatic reaction. Further reduction of enzyme-substrate contact time is not feasible because that would require an impractically high voltage or a buffer condition unsuitable for enzyme assay. A two-step method (Figure 1) with sodium salicylate as internal standard (IS) was devised to circumvent this problem. First, a large plug of LDH solution containing 1mM IS was injected into the capillary and the LDH concentration was first calibrated with IS by their relative peak area. Then the enzyme solution was diluted with running buffer (without IS) and a small plug was injected for assay. Dilution affords a fresh enzyme solution for each parallel assay, avoiding possible contamination. Furthermore, a diluted enzyme solution was used to ensure relatively small and consistent reagents consumption and keep the reaction in the linear region.

Ensemble average activity of crystal LDH

Two crystals, *a* and *b,* from droplet D (Figure 2A) were isolated broken apart individually, and three pieces from each crystal (Figure 2B) were tested. The results are very interesting. First, reproducibility better than 2.0% relative standard deviation (RSD) was obtained on all six crystal fragments with three parallel assays each. Second, activity of fragments from the same crystal showed 0.6% and 2.0% RSD for crystal *a* and *b* respectively, indicating the homogeneity of the crystals. The fragments are plotted in the order of being picked from the crystallization droplet. The microliter size droplet dries quickly once removed from the crystallization chamber and exposed to air. Breaking crystals and picking up the fragments took up to a few minutes to complete. Crystals *a* and *b* were first isolated into an even smaller droplet to ensure the

fragments picked up were from the same crystals. By the time the last fragments (*a3* and *b3*) were picked, clear depositions on the fragments, presumably components from the solution, including LDH, were observed. Washing with clear solution greatly reduced these depositions; however the rest were inevitably transferred with the crystal for dissolving. This is attributed to the observed higher than average activity for fragments *b3* and the lower than average activity for fragments *a3*. Third, T-test shows significant difference ($P<0.05$) between all nine measurements of activity of crystal *a* and those of crystal *b*.

Figure 3A plots the activity of all 21 crystals obtained from five droplets. Heterogeneity of LDH activity from different crystals is evident. Droplet A, B, C and D are of the same initial condition (35% PEG 400 and 8% PEG 4000 (v/v)); droplet E are of 34% PEG 400 and 8% PEG 4000 (v/v). Although only a limited number of crystals were tested, this slightly different crystallization condition does not seem to affect the resulting crystals' activity ($P=0.12$). Crystal size does not correlate with either activity (correlation coefficient 0.07) or the precision of the assay (correlation coefficient 0.13). Histogram (Figure 3B) shows the activity of crystal LDH is not continuous but rather falls into discrete levels. This correlates with previous X-ray crystallography results that crystallization separate different conformations of LDH.

Single molecule activity of crystal LDH

Although LDH crystals showed significant difference in their average activity, single molecule assay was necessary to determine whether individual molecules from the same crystal have identical activities. Previous single molecule experiments showed that LDH molecules from solution have different activities[2]. Slightly different experimental conditions were used here. Heterogeneity of LDH molecules directly from solution (without crystallization) was

nevertheless observed (Figure 4A). In contrast, LDH from the same crystal showed much narrower activity distribution (Figure 4B). This narrow activity distribution was observed for all four crystals tested (Figure 5). F-test indicates the activity variance is significantly different ($P<0.05$) between LDH directly from solution and those from any crystal source. The variation (relative standard deviation) of activity for LDH from the same crystal is about 10% or better, whereas 26% is observed for LDH directly from solution. Precision of experiment, although not tested here, is not expected to be better than the 9% obtained on similar systems for repeated incubation of the same molecule[14]. So molecules from the same crystals are likely to be identical in activity within experimental error. Furthermore, the single molecule activity are significantly different among crystals ($P<0.05$) except for crystal *1* and *4* ($P=0.26$). This agrees with our ensemble average experiments results that crystal activities seem to fall into a few distinct levels.

Since only a limited number of crystals are picked and crystallization itself is a selective process, it was still not clear whether the heterogeneity of LDH directly from solution, which is purified by commercial sources, arises from conformational heterogeneity. Experiments were attempted to see whether activity distribution of dissolved crystal LDH might broaden after storage at 37 °C. Figure 6A shows that after a week at 37 °C, LDH molecules from crystal *2* changed significantly ($P<0.05$). It is worth noting that the other portion stored at -80 °C showed only minor change ($P=0.65$) from the portion assayed a week earlier. This not only shows that that -80 °C storage preserves the enzyme but also the performance of system is reliable and the difference of average activity observed between crystals are not artifacts caused by instrumental fluctuations. For crystal *3* (Figure 6B), change, although much less significant ($P=0.17$) comparing to change of crystal *2*, was also observed after 2 weeks at 37 °C, and much less

change (P=0.09) after 2 weeks at -80 °C. The gradual broadening of activity distribution of crystal *4* was evident over the course of 48 hours (Figure 6C). The average activity, however, stayed virtually unchanged.

Figure 6D shows the overall activity changes of all 3 crystals. In all cases, the distribution widened after storage at -80 °C. But the changes in average activity were not uniform: the activity of crystal *2* decreased; that of crystal *3* increased, and that of crystal *4* stayed virtually unchanged. The significant increase of the average activity of crystal 3 means the observed changes were not caused by thermal or proteolytic damages to the LDH molecules, but rather by conformational randomization. This further supports the argument that the multiple conformations observed in crystals are not artifacts of crystallization but a reflection of conformational multiplicity in solution. A closer examination of the results reveals that both the average activities and the distributions tend to mimic those of the LDH from solution source, suggesting equilibrium among different conformations of LDH molecules. The equilibrium is apparently a slow process, and certain conformation, such as that of crystal *3*, is much more stable than the others. The heterogeneity of single molecule activity of the solution LDH can largely be explained by the slow equilibrium among different conformations.

Conclusions

An electrophoresis based method was applied to compare the specific activity of LDH from different micro-crystals. Ensemble average assay of LDH from crystals showed that they fall into distinct groups in terms of catalytic activity. Single molecule activities are similar among LDHs from within a crystal and significantly different among those directly from

solution. Crystal single LDH molecule activities distribution tends to mimic that of solution origin after dissolving and storage at 37 °C.

Our previous X-ray crystallography results showed that multiple conformations of LDH active site loops exist in LDH crystals. These active site loop conformations can vary both among crystal LDH and among the subunits of the same crystal LDH. The experiments here demonstrated that conformation multiplicity exists in solution state, and slow equilibrium among these conformations in solution is responsible for the observed static heterogeneity of LDH activity.

Acknowledgement

E.S.Y. thanks the Robert Allen Wright Endowment for Excellence for support. We thank Dr. Mary Jo Schmerr for her valuable help in the ensemble assay study. The Ames Laboratory is operated for the U.S. Department of Energy by Iowa State University under Contract No. W-7405-Eng-82. This work was supported by the Director of Science, Office of Basic Energy Sciences, Division of Chemical Sciences.

References

(1) Anfinsen, C. B. *Science (Washington, DC, U. S.)* **1973**, *181*, 223-230.

(2) Xue, Q.; Yeung, E. S. *Nature (London, U. K.)* **1995**, *373*, 681-683.

(3) Tan, W.; Yeung, E. S. *Anal. Chem.* **1997**, *69*, 4242-4248.

(4) Nichols, E. R.; Gavina, J. M. A.; McLeod, R. G.; Craig, D. B. *Protein J.* **2007**, *26*, 95-105.

(5) Craig, D. B.; Arriaga, E.; Wong, J. C. Y.; Lu, H.; Dovichi, N. J. *J. Am. Chem. Soc.* **1996**, *118*, 5245-5253.

(6) Ashley C. Dyck, D. B. C. *Luminescence* **2002**, *17*, 15-18.

(7) Craig, D. B.; Nachtigall, J. T.; Ash, H. L.; Shoemaker, G. K.; Dyck, A. C.; Wawrykow, T. M. J.; Gudbjartson, H. L. *J. Protein Chem.* **2003**, *22*, 555-561.

(8) Lu, H. P.; Xun, L.; Xie, X. S. *Science (Washington, DC, U. S.)* **1998**, *282*, 1877-1882.

(9) Edman, L.; Foldes-Papp, Z.; Wennmalm, S.; Rigler, R. *Chem. Phys.* **1999**, *247*, 11-22.

(10) Zhuang, X.; Kim, H.; Pereira, M. J. B.; Babcock, H. P.; Walter, N. G.; Chu, S. *Science (Washington, DC, U. S.)* **2002**, *296*, 1473-1476.

(11) van Oijen, A. M.; Blainey, P. C.; Crampton, D. J.; Richardson, C. C.; Ellenberger, T.; Xie, X. S. *Science (Washington, DC, U. S.)* **2003**, *301*, 1235-1238.

(12) Velonia, K.; Flomenbom, O.; Loos, D.; Masuo, S.; Cotlet, M.; Engelborghs, Y.; Hofkens, J.; Rowan, A., E.; Klafter, J.; Nolte, R. J. M.; de Schryver, F. C. *Angew. Chem., Int. Ed.* **2005**, *44*, 560-564.

(13) Flomenbom, O.; Velonia, K.; Loos, D.; Masuo, S.; Cotlet, M.; Engelborghs, Y.; Hofkens, J.; Rowan, A. E.; Nolte, R. J. M.; Van der Auweraer, M.; de Schryver, F. C.; Klafter, J. *Proc. Natl. Acad. Sci. U. S. A.* **2005**, *102*, 2368-2372.

(14) Shoemaker, G. K.; Juers, D. H.; Coombs, J. M. L.; Matthews, B. W.; Craig, D. B. *Biochemistry* **2003**, *42*, 1707-1710.

(15) Hatzakis, N. S.; Engelkamp, H.; Velonia, K.; Hofkens, J.; Christianen, P. C. M.; Svendsen, A.; Patkar, S. A.; Vind, J.; Maan, J. C.; Rowan, A. E.; Nolte, R. J. M. *Chem. Commun.* **2006**, 2012-2014.

(16) Hsin, T. M.; Yeung, E. S. *Angew. Chem., Int. Ed.* **2007**, *46*, 8032-8035.

(17) Frauenfelder, H.; Sligar, S. G.; Wolynes, P. G. *Science (Washington, DC, U. S.)* **1991**, *254*, 1598-1603.

(18) Yang, H.; Luo, G.; Karnchanaphanurach, P.; Louie, T.-M.; Rech, I.; Cova, S.; Xun, L.; Xie, S. X. *Science (Washington, DC, U. S.)* **2003**, *302*, 262-266.

(19) Min, W.; Luo, G.; Cherayil, B. J.; Kou, S. C.; Xie, X. S. *Phys. Rev. Lett.* **2005**, *94*, 1983021-1983024.

(20) Li, C.-B.; Yang, H.; Komatsuzaki, T. *Proc. Natl. Acad. Sci. U. S. A.* **2008**, *105*, 536-541.

(21) Kuznetsova, S.; Zauner, G.; Aartsma, T. J.; Engelkamp, H.; Hatzakis, N.; Rowan, A. E.; Nolte, R. J. M.; Christianen, P. C. M.; Canters, G. W. *Proc. Natl. Acad. Sci. U. S. A.* **2008**, *105*, 3250-3255.

(22) Vallurupalli, P.; Kay, L. E. *Proc. Natl. Acad. Sci. U. S. A.* **2006**, *103*, 11910-11915.

(23) Polakowski, R.; Craig, D. B.; Skelley, A.; Dovichi, N. J. *J. Am. Chem. Soc.* **2000**, *122*, 4853-4855.

(24) Bao, J.; Regnier, F. E. *J. Chromatogr., A* **1992**, *608*, 217-224.

(25) Regnier, F. E.; Patterson, D. H.; Harmon, B. J. *Trac-Trend. Anal. Chem.* **1995**, *14*, 177-181.

(26) Bao, J. J.; Fujima, J. M.; Danielson, N. D. *J. Chromatogr., B: Anal. Technol. Biomed. Life Sci.* **1997**, *699*, 481-497.

(27) Van Dyck, S.; Kaale, E.; Nováková, S.; Glatz, Z.; Hoogmartens, J.; Van Schepdael, A. *Electrophoresis* **2003**, *24*, 3868-3878.

(28) Novakova, S.; Van Dyck, S.; Van Schepdael, A.; Hoogmartens, J.; Glatz, Z. *J. Chromatogr., A* **2004**, *1032*, 173-184.

(29) Glatz, Z. *J. Chromatogr., B: Anal. Technol. Biomed. Life Sci.* **2006**, *841*, 23-37.

(30) Li, F. Ph.D., Iowa State University, Ames, Iowa, 2006.

Table 1: Single molecule measurement size.

Source	Number of molecules measured
Solution	14
Crsytal 1	21
Crsytal 2	23
Crsytal 3	17
Crsytal 4	25
Crystal 2 after 1 week at 37 °C	25
Crystal 2 after 1 week at -80 °C	13
Crystal 3 after 2 weeks at 37 °C	23
Crystal 3 after 2 week at -80 °C	14
Crystal 4 after 12 hours at 37 °C	27
Crystal 4 after 24 hours at 37 °C	26
Crystal 4 after 48 hours at 37 °C	26

Figure captions

Figure1. Ensemble assay of LDH. (A): Calibration of LDH against internal standard (IS) salicylate. 0.2psi, 30sec injection of LDH solution containing 1mM IS. (B): Assay of diluted LDH solution by EMMA. 0.1psi, 10sec injection of diluted LDH solution.

Figure 2. Ensemble assay of fragments from two crystals of the same mother liquor. (A): Polarizing micrograph of the two crystals. (B): Relative activity of individual crystal fragments. Column height is the average of three replica runs. Error bars stand for 2σ.

Figure 3. (A): Relative activity of 21 crystals obtained from five crystallization droplets. Droplet A, B, C, and D were of 35% PEG 400 and 8% PEG 4000 (v/v); droplet d was of 34% PEG 400 and 8% PEG 4000 (v/v). Column height is the average of three replicas except for droplet D where all nine data from three crystal fragments are used for both crystals. Error bars stand for 2σ. (B): Histogram of relative activity of the crystals.

Figure 4. Single molecule assay of LDH. (A): ~4×10^{-16}M LDH directly from solution. (B): ~5×10^{-16}M (estimated) LDH from a crystal. (C): Blank without any LDH. All incubations are 1 hour at 40 °C with PH 9.0 buffer containing 20mM TrisHCl, 3mM L-lithium lactate, and 1mM NAD+.

Figure 5. Activity of single LDH molecules from different sources. Column height is the average of all measured molecules from the same source. See Table 1 for measurement size. Error bars stand for 2σ.

Figure 6. Activity changes of single LDH molecules from three crystals. (A): Crystal *2* after 1 week in -80 °C and 37 °C; (B): Crystal *3* after 2 weeks at -80 °C and 37 °C; (C): Crystal *4* after 12, 24, and 48 hours at 37 °C; (D): Crystal *2*, *3*, and *4*, before and after storage at 37 °C storage vs. those directly from solution. Column height is the average of all measured molecules from the same source. See Table 1 for measurement size. Error bars stand for 2σ.

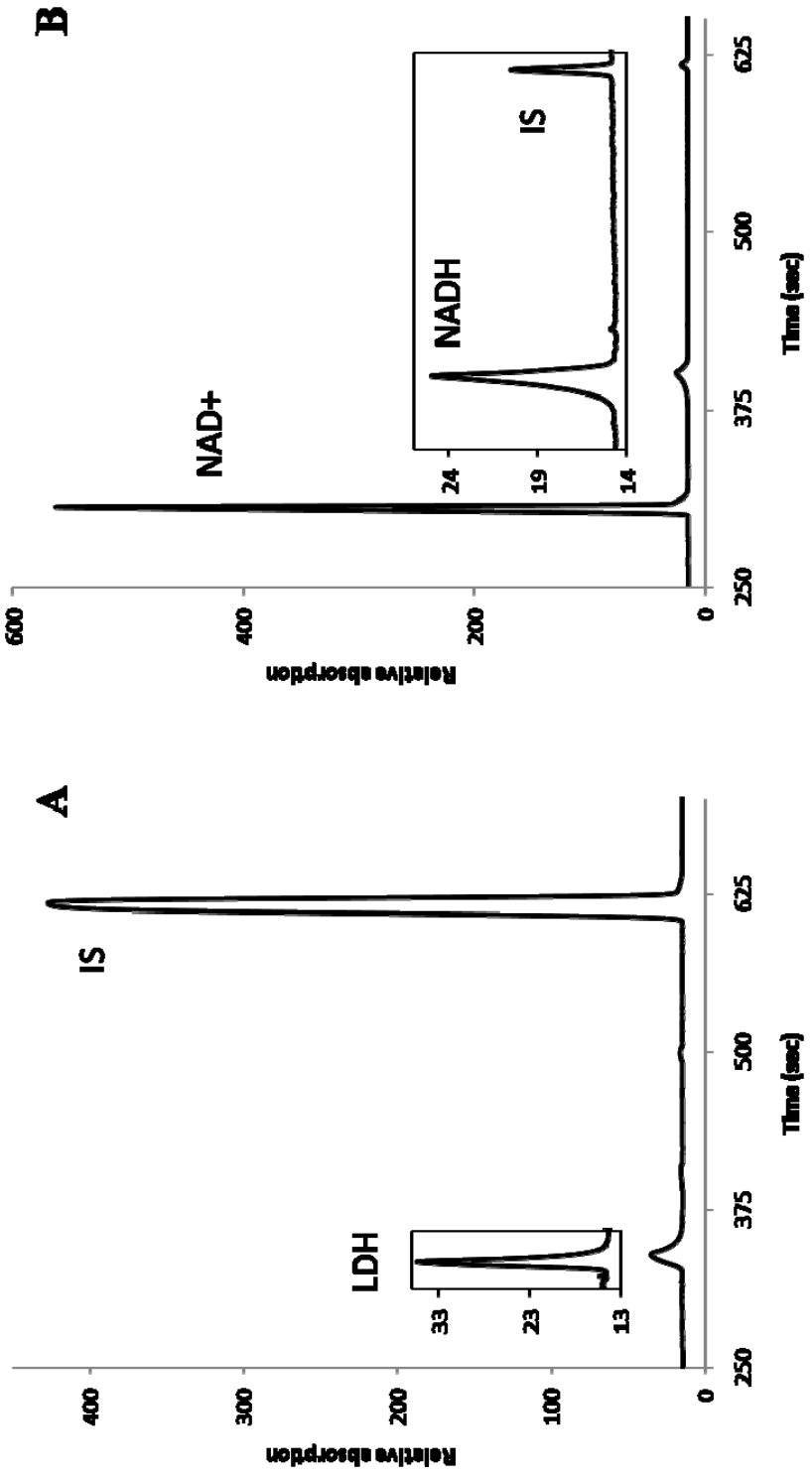
A
IS
LDH
33
23
13
Relative absorption
Time (sec)
B
NAD+
NADH
IS
24
19
14
Relative absorption
Time (sec)

Figure1

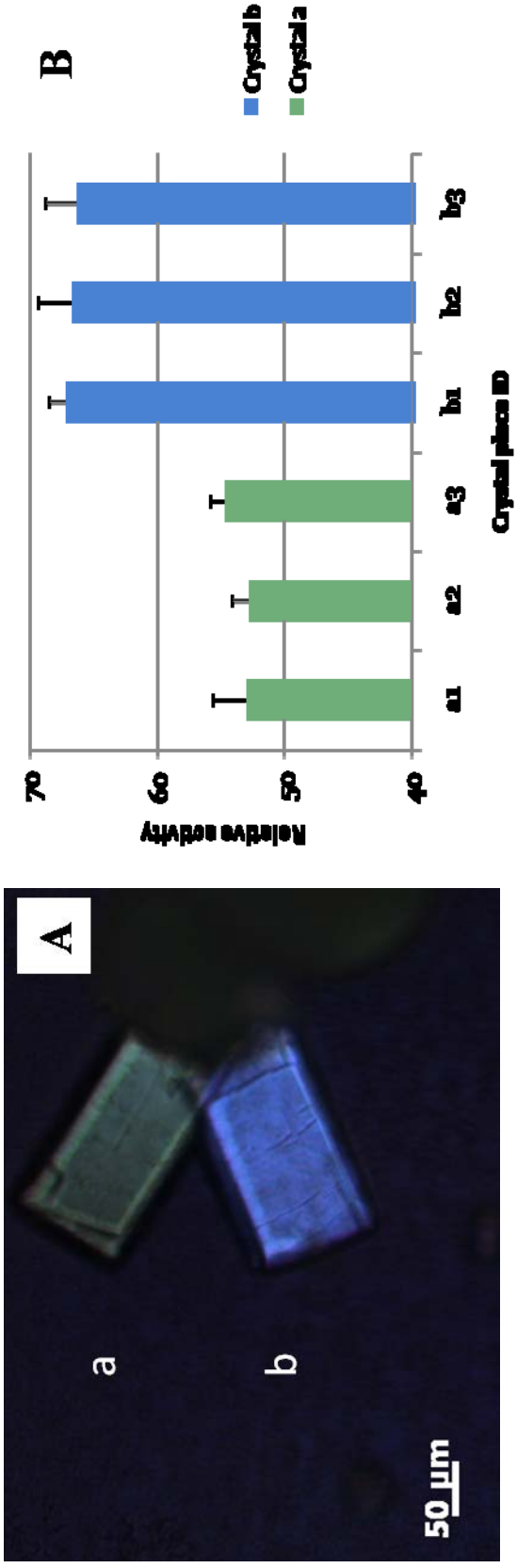
A
a
b
50 μm
B
Crystal b
Crystal a
Relative activity
70
60
50
40
a1
a2
a3
b1
b2
b3
Crystal plane ID

Figure2

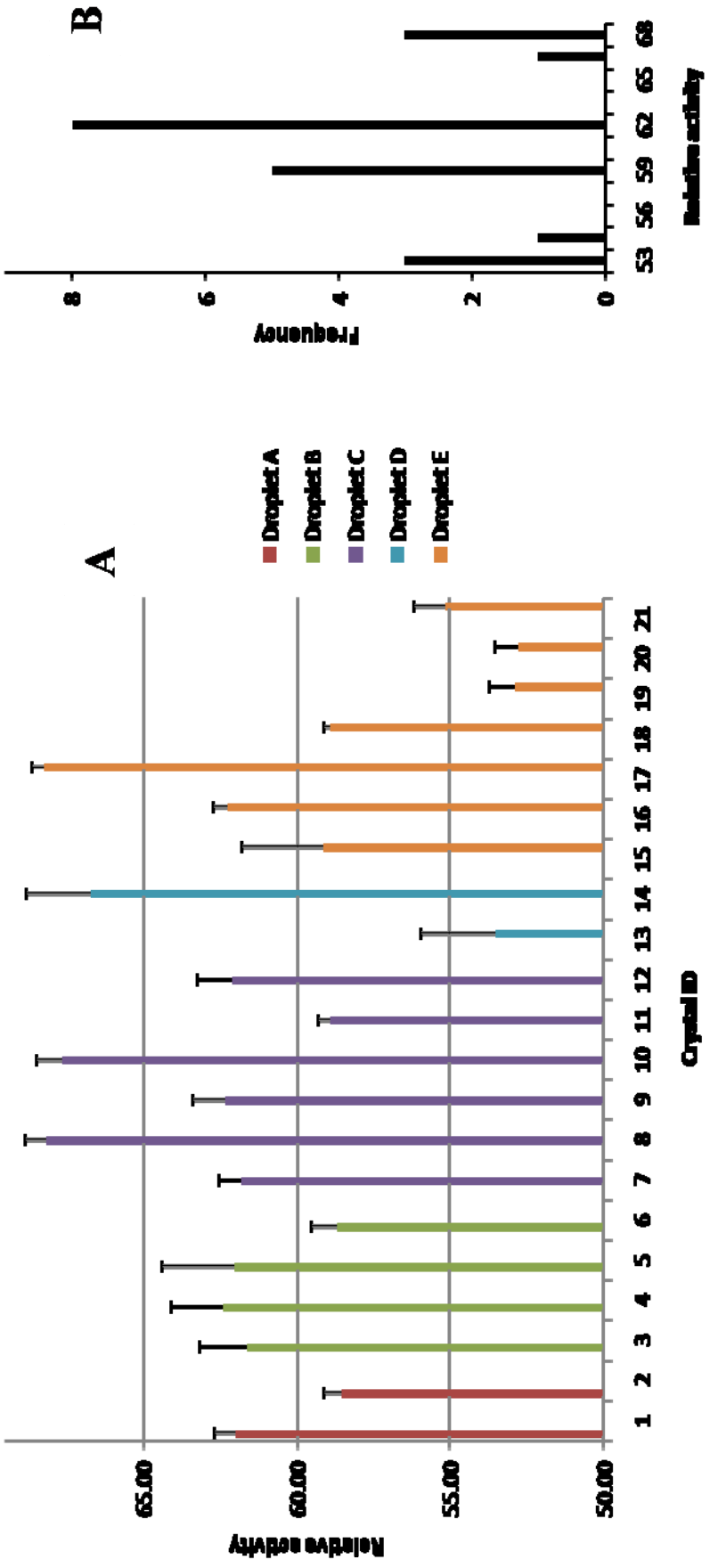
A
Droplet A
Droplet B
Droplet C
Droplet D
Droplet E
Relative activity
65.00
60.00
55.00
50.00
Crystal ID
1 2 3 4 5 6 7 8 9 10 11 12 13 14 15 16 17 18 19 20 21
B
Frequency
0 2 4 6 8
Relative activity
53 56 59 62 65 68

Figure3

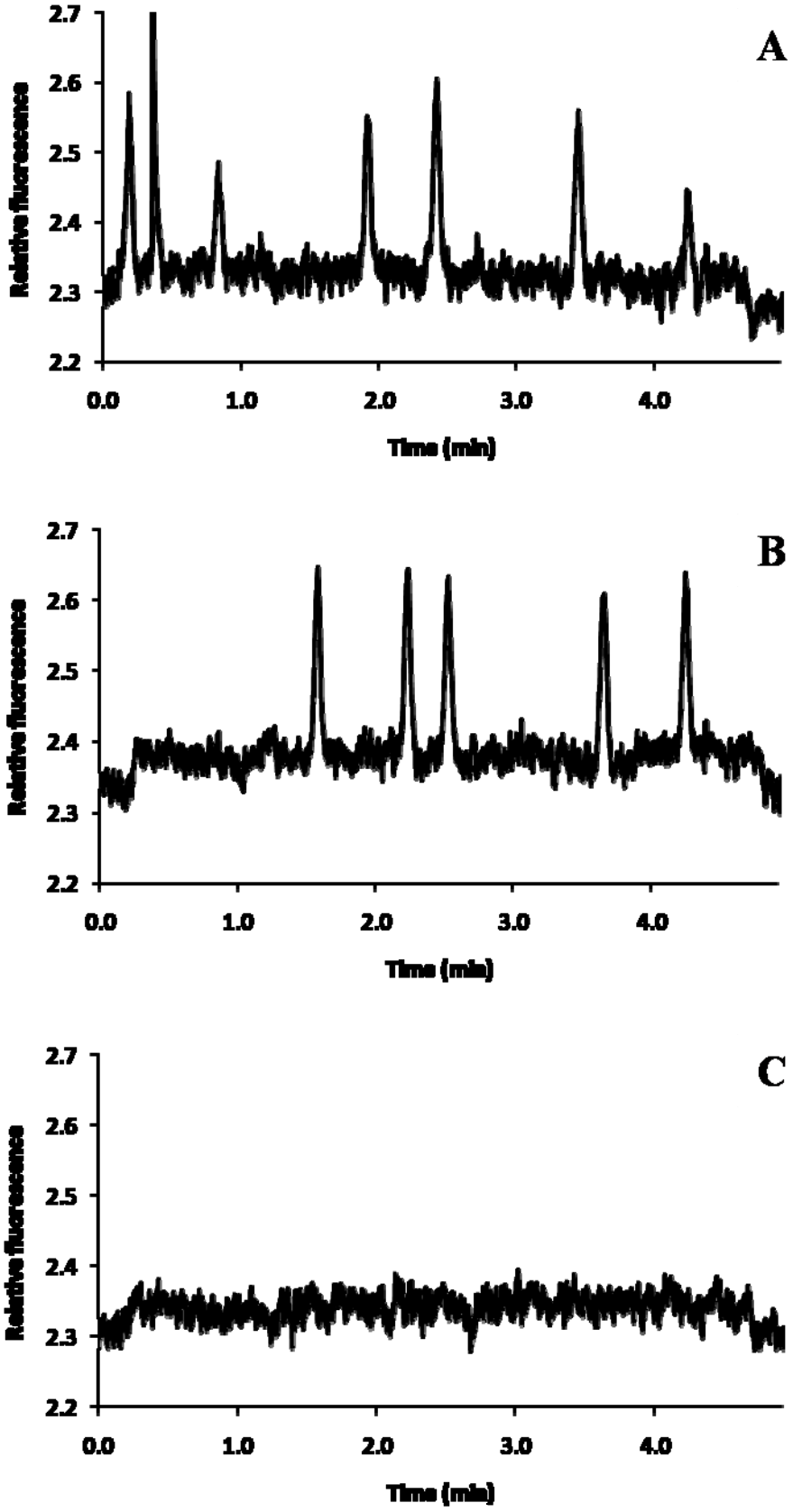
A
Relative fluorescence
2.7
2.6
2.5
2.4
2.3
2.2
0.0
1.0
2.0
3.0
4.0
Time (min)
B
Relative fluorescence
2.7
2.6
2.5
2.4
2.3
2.2
0.0
1.0
2.0
3.0
4.0
Time (min)
C
Relative fluorescence
2.7
2.6
2.5
2.4
2.3
2.2
0.0
1.0
2.0
3.0
4.0
Time (min)

Figure 4

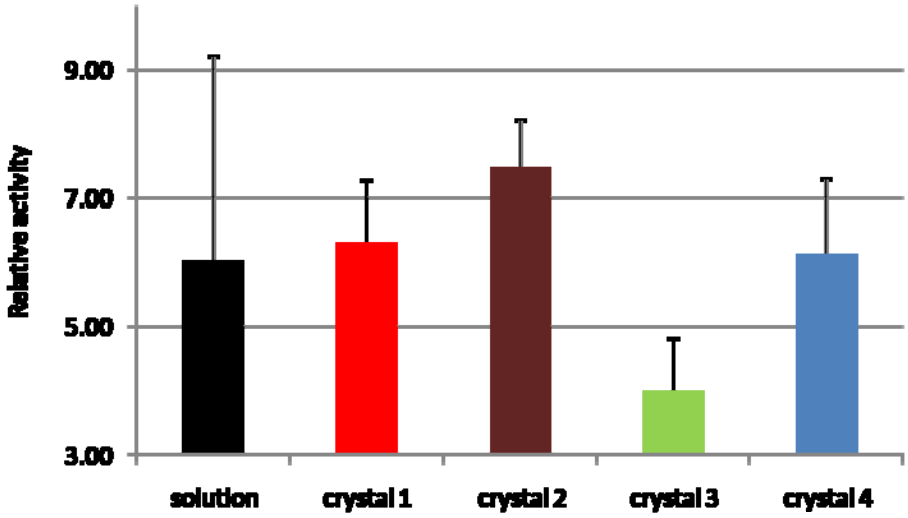
Relative activity
9.00
7.00
5.00
3.00
solution
crystal 1
crystal 2
crystal 3
crystal 4

Figure 5

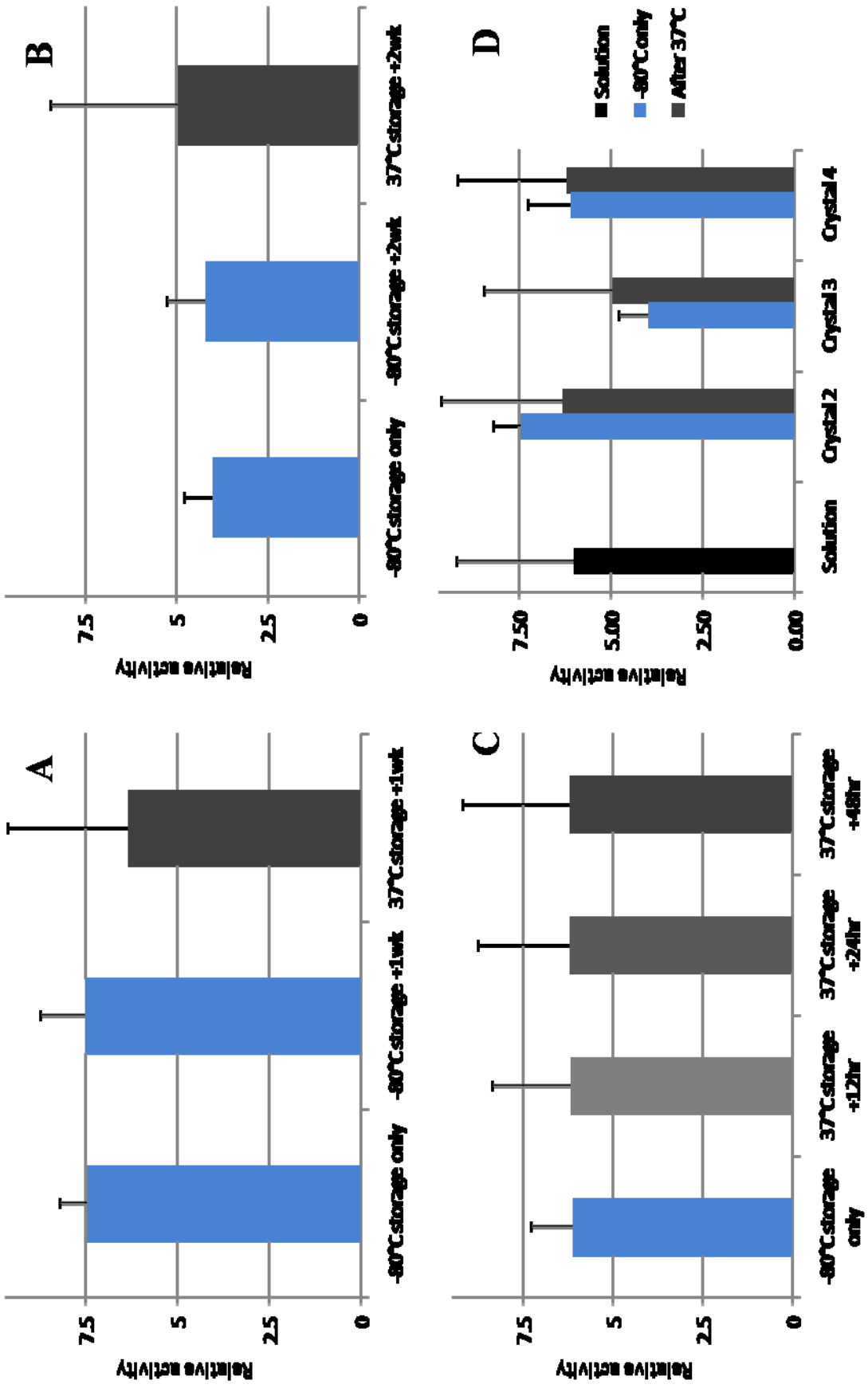
A
B
C
D
Relative activity
7.5
5
2.5
0
7.50
5.00
2.50
0.00
-80°C storage only
-80°C storage +1wk
37°C storage +1wk
-80°C storage +2wk
37°C storage +2wk
37°C storage +12hr
37°C storage +24hr
37°C storage +48hr
Solution
Crystal 2
Crystal 3
Crystal 4
Solution
-80°C only
After 37°C

Figure 6

CHAPTER 5. GENERAL CONCLUSIONS

Electrophoresis has been an instrumental analytical tool in helping biologist getting new information; it is also the incessant biological inquiries that continue to prompt analytical chemists to produce better analytical tools. With the success of the genomic era behind, biologic research now moves on into the new field of proteomics and metabolomics. Continuous development of electrophoresis instrumentation and application is essential to keep this magnificent tool up to date with the level of scientific quest in biology.

Two-dimensional gel electrophoresis currently offers the best general approach to proteomic scale analysis. The development of a fully automated instrument would greatly improve its reproducibility, shorten its duty cycle, and reduce the cost of full scale proteomic research. Hopefully, the prototype design presented in this study may soon see its fully automated version and find excitation application in research and clinical laboratories. Although the native fluorescence approach can be very efficient in fast and automated gel protein detection, it may be insufficient when positive protein identification is required. It is interesting to see whether mass spectrometry can be effectively coupled to two-dimensional gel electrophoresis for automated protein identification.

The capillary format not only freed electrophoresis from supporting matrices, but also found it many great applications in micro-bioanalysis. The ability of CE to analyze the micro-environment was applied in this work to study the change of metabolites levels in cells in response to external stimuli, and to investigate the subtle details of enzyme conformation and catalytic property. These studies provide exciting new information to biologists and chemists alike and will likely to promote further research in their respective fields. As these research areas

move forward, it is likely that a high-throughput sample preparation interface will be developed to take full advantage of the massive capability of the automated capillary array electrophoresis instruments.

ACKNOWLEGEMENT

This work would not be imaginable without the support of so many great people that I came to know in the few years at Iowa State. My deepest appreciation goes to my advisor, Dr. Edward S. Yeung. He is a devoted scientist and a great mentor. His brilliance is so dazzling yet his manner is always so humble. His care and guidance helped through all these years and his enthusiasm and optimism will always inspire me to reach higher.

I would also like to acknowledge the support of Dr. Houk, Dr. Lin, Dr. Petrich, Dr. Porter, Dr. Smith, and Dr. Tabatabai for kindly serving on my committee and for all the guidance.

My appreciation also goes to the talented Yeung group members for their great help and friendship: Dr. Dragon Isailovic, Slavica Isailovic, Dr. Jiyong Lee, Dr. Hungwing Li, Guoxin Lu, Dr. Tse-min Hsin, Jiangwei Li, Yun Zhang, Wei Sun, and Dr. Ning Fang. I want specially thank my collaborators Wenjun Xie, Dr. Fenglei Li, Dr. Wei Wei, Dr. Sangwon Cha, Dr. Hui Zhang, and Dr. Chanan Sluszny, for their direct assistance to my research.

I want also thank my extended family on the other side of the globe. Their endless cares and forever encouragement is what motivate me all along.

Finally, I want to thank my wonderful wife, Chun, who made me all for the better with her patience, enthusiasm, intelligence, and endless love. Sharing my life with her is the best thing ever happened to me.